2012-11-27

Internal multiple prediction: an application on synthetic data, physical modeling data and field data

Hernandez, Melissa

UNIVERSITY OF CALGARY

Internal multiple prediction: an application on synthetic data, physical modeling data and field data

by

Melissa Judith Hernandez Quijada

A THESIS

SUBMITTED TO THE FACULTY OF GRADUATE STUDIES

IN PARTIAL FULFILMENT OF THE REQUIREMENTS FOR THE

DEGREE OF MASTER OF SCIENCE

DEPARTMENT OF GEOSCIENCE

CALGARY, ALBERTA

NOVEMBER, 2012

Abstract

In this work we examined and applied a method of internal multiple prediction based on the inverse scattering series. The internal multiple prediction algorithm predicts and then suppresses all order of internal multiples independent of the subsurface reflectors that generate them. In this thesis we promote a stepped approach to predicting multiples in a given field data set: first, by carrying out synthetic/numerical examples; second by carrying out tests on laboratory physical modeling data; and finally by testing prediction of a field data set suspected to be strongly contaminated with internal multiples. In the synthetic examples we draw conclusions about the central frequency of the seismic wavelet and the optimum choice for parameter epsilon (ϵ). The physical modelling study, in which internal multiples are deliberately generated in order to be predicted, is the first of this kind. The results confirm the synthetic's study conclusions regarding the estimation of epsilon (ϵ), and motivated the development of a method for optimum estimation of epsilon (ϵ) based on autocorrelation. In the land data study, the prediction allows us to confirm and precisely predict the presence of internal multiples in regions where they were expected.

Acknowledgements

I would like to thanks to my supervisor, Dr. Kris Innanen for his guidance, wise suggestions support and kind words during the master. Thank to Dr. Donald Lawton and Dr. Joe Wong for their suggestions and comments.

Special thanks to Nexen Inc. for donated the well and seismic data, especially to Eric Von Lunen.

Thank to all the directors and staffs of CREWES, especially Kevin Hall, Rolf Maier, and Laura Baird.

Moreover, I would like to express my recognition and acknowledgements to my fellow students and friends that help me during the realization of this thesis, Diane Lespinasse, Heather Lloyd, and Steve Kim.

Dedication

To my beloved Parents and my aunt Nieves

Table of Contents

List of Tables

List of Figures and Illustrations

List of Symbols, Abbreviations and Nomenclature

Symbol	Definition
FSM	Free surface multiple
IM	Internal multiple
b_{3im}	Predicted internal multiple
k_z	Pseudo depth wavenumber
z	Pseudo depth
b_1	Seismic data after transformations
z_1'	Pseudo depth of the first event
z_2'	Pseudo depth of the second event
z_3'	Pseudo depth of the third event
ϵ	Epsilon
D	Measured surface data
x_g	Position of the receiver
x_s	Position of the source
t	Time
ω	Frequency
SE_1	Subevent 1
SE_2	Subevent 2
SE_3	Subevent 3
t_1	Travel time of the first interface
t_2	Travel time of the second interface
R_1	Coefficient of Reflection 1
R_2	Coefficient of Reflection 2
T_1	Coefficient of transmission 1
T_1'	Coefficient of transmission 1 (negative)
NMO	Normal Moveout
tau	Intercept in time
p	Ray parameter
x-t	offset-time
K-L	Karhunen-Loeve
tau-p	Intercept in time-ray parameter

Chapter One: Introduction

The seismic reflection method (Telford, W.M., Geldart, L.P., and Sheriff, R.E., 1990) is considered one of the most important geophysical methods, as it provides an approximate image of the subsurface; it is typically applied in exploration seismology at regional scale or to delineate the architecture of a reservoir. In seismic surveying, a ground movement is produced by a seismic source (dynamite, vibroseis, air gun, thumper) and a geophone located at some distance apart laterally intercepts and records the signal. Seismic surveys involve hundreds or thousands of seismic experiments: one source shot that is recorded in several receivers, and then the source and receivers are moved to another location.

Measurements at the receiver record the arrival of refractions, primaries reflections and noise. Refractions refer to seismic events that cross the interface and the return to the receiver. Primary reflections are events which experience a single reflection in the subsurface. A reflection profile or structural image of the subsurface across a certain area can be constructed from the arrival of these primaries reflections. Noise is also present in the seismic record masking the primary reflections. Multiples are a source of coherent noise, and in practice multiples reflections are observed as well as primaries, and is difficult to distinguish between them. Seismic multiples are events which undergo more than once change in vertical propagation direction as they travel from the source to the receiver (Weglein, A., and Dragoset, 2005).

Generally, there are two types of multiples: free surface multiples and internal multiples. A free surface multiple (FSM) is an event that has at least one reflection at the Earth-air or water-air boundary. An internal multiple instead has all of its downward reflections below the free surface.

Free surface multiples are more common than internal multiples. However, interbed multiples can be more problematic because they mask information from seismic data, especially in more sophisticated analysis such as AVO (Alvarez and Larner, 1996; and Foster and Mosher, 1992.). Additionally, there is often very little difference in moveout velocities between primaries and short period internal multiples which makes it harder to distinguish between them.

Different techniques have been developed to attenuate or suppress both free surface and internal multiples. In the next section we will discuss some of them, and their advantages and disadvantages.

1.1 Previous work/background

1.1.1 Conventional methods

Sloat (1948) was one of first scientists that identified seismic multiples or echo reflections in seismic data. Since then several methods have been presented to suppress or attenuate these events.

Conventional multiple attenuation methods fall into three main categories: 1) Approaches that take advantage of the periodicity of the multiples; 2) Methods based on the difference of NMO, and 3) Wave equation methods.

Backus (1959) was probably the first to show that multiples have a periodic character. This characteristic can be used to distinguish them from primaries. Multiples usually are periodic because arrive many times whereas primaries only arrive once for each reflector. This technique requires that multiples have to be periodic, but not the primaries. This condition is satisfied just at zero offset, but is less effective with increasing offset. The transform tau-p can be applied in to extend the method to all offsets (Trinks, 2000). An example of this method is predicted or gapped deconvolution (Yilmaz, 1987; Yan, 2002). This method uses a statistical approximation based on least squares approach. This method is useful in suppressing short–period free–surface multiples generated at shallow reflectors.

The second group uses filtering techniques, taking advantage of the different moveout of multiple reflections compared to primary reflections at the same time position. Multiples tend to have more moveout (curvature as function of the source-receiver offset) than primaries reflections, i.e., multiples moveout velocities are lower than primaries at the same arrival time, because multiples have more of their travel path in shallower portions of the earth. Since velocity generally increases with depth, multiples have a lower moveout velocity than primaries. This difference in moveout is more noticeable at far offsets.

These filtering methods can successfully suppress multiples generated at moderate to deep reflectors where multiples are well–separated from their primaries. However, their application to real data can lead to disappointing results. A significant moveout difference must exist between primaries and multiples to obtain an effective result, and these methods can fail in muted zones (Yilmaz, O., 1987).

There are two techniques that take advantage of the difference in moveout: Radon Transform (tau-p) and Karhunen-Loeve (K-L) Transform. *The Radon Transform* models linear and hyperbolic events. The seismic data in time-offset domain is transform to **tau-p** domain, where **tau** is intercept in time and **p** is the ray parameter (Yan, 2002). Events that are difficult to separate in x-t domain such as direct arrival, and ground roll, can be well distinguished in the tau-p domain, because they have different incidence angles (p). The data in the time-offset (t-x) domain is summed along lines or hyperboles to yield points in the tau-p domain. So, the events would look like isolated points in the Radon domain. Then, the undesirable events could be selectively filtered from the data. Finally, the inverse Radon transform is applied to reconstruct the data in time-offset (t-x) domain, Margrave (1999).

The Karhunen-Loeve (K-L) transform has been used for multiple suppression in multi-channel seismic data since the 1980's (Jones and Levy, 1987). This method extracts coherent information from seismic data, so it is requires that the multiples events possess a trace-trace coherency. The attenuation of multiples is realized by isolating coherent energy from incoherent energy.

The third group of methods, wavefield prediction and subtraction, are based on the wave equation. They use recorded data to predict multiples by wave extrapolation or inversion procedures. These wavefield methods can suppress all multiples generated by any complex system of reflectors, as long as the recorded wavefield has complete internal physical consistency between primaries and multiples (Xiao, C., Bancroft, J., Brown, J., and Cao, Z., 2003). These methods require a robust set of data because the lack of data causes inaccuracy in the prediction of multiples (Trinks, 2000).

Conventional methods assume that the earth is one dimensional, the velocity is known, multiples are periodic and primaries not, or that enough differential moveout exists between primaries and multiples. In most of the cases these assumptions are valid and conventional methods are apply effectively. In complex areas such as: dipping reflectors, decreases in velocity with depth, where these assumptions are violated, conventional methods are not successful. In these cases unconventional methods are needed to overcome these limitations.

1.1.2 Unconventional methods

The attenuation of free surface multiples has been studied by Verschuur et al., 1992; Fokkema and Van den Berg (1990); Weglein, Carvalho, and Stolt (1992). The method of Verschuur (1992), is based on Huygen's model of seismic wave propagation, is a surface replacement approach.

Fokkema and Van den Berg (1993) method is derived from reciprocity theorem in integral form and results a Neumann series representation. These methods do not require information of the earth model.

Weglein, Carvalho and Stolt (1992) developed a method to remove free surface multiples using inverse scattering series. This method removes all orders of free surface multiples, and does not touch the primaries. The requirements for this technique are: knowledge of the source wavelet and the data must contain near offsets. The inverse scattering free surface multiple removal describes the wave propagation using a scatterer model with a reference medium where the waves interacts with different scattering points. This method assumes that the sources and receivers are placed in the water and that the multiples are generated by an acoustic free surface above the sources and receivers. Coates and Weglein (1996) found later that this method also suppress internal multiples which contain S phases (elastic background). The ability to remove converted internal multiples is important in salt structures because in these types of settings conversion can occur considerably.

There are also methods that attenuate or remove internal multiples. Verschuur et al. (1991) have adapted their surface multiple removal scheme to remove internal multiples. In this method, first remove all free surface multiples, and then downward continue the data to the next reflector, the multiples associated with the new datum are then removed in analogy with free surface removal. This is a "stripping" approach that requires velocity information of the layers and strong reflectors.

Verschuur et al., in 1992 proposed a surface related multiple elimination method (SRME). This method considers that the combination of two primaries could generate a free surface multiple. The final result can be achieved by combining all possible reflection points at the surface. This method uses the cross-convolution of the seismic measurements in order to predict free surface multiples and then the adaptive subtraction to remove them from seismic data.

A Jakubowicz (1998) used the wave equation migration to model internal multiples. Moreover this method utilized implicitly a version of the generalized Bremmer series (De Hoop, 1996). In the Bremmer series the wavefield is split into parts: up-going and down-going constituents, then reflections and transmissions operators coupled both parts. The first term of the series represents the direct wave, the second term models reflection or transmission, and so on. Malcolm (2005) used a hybrid of the Bremmer and Lippmann-Schwinger series to estimate artifacts caused by internal multiples.

The Lippmann-Schwinger series was first proposed by Lippmann in 1956. Through this series the wave equation is solved in a known background or reference model. The Green's operator is used as contrast operator, represents the difference between the reference or known operator and the same operator in the true model. Then Moses (1956); Prosser (1969); and Razavy (1975) developed this idea further for the quantum scattering problem and wave equation. Araujo et al. (1997) implemented the inverse scattering series to develop techniques for both surface and internal multiples attenuation. This method is

capable of attenuating internal multiples without any a priori information about the medium through which the waves propagate, i.e., is a data-driven process. Furthermore, the primaries reflections remain untouched.

Moreover, the prediction of internal multiple based on inverse scattering series was investigated by Araujo et al (1994). In this work we investigate an application of Weglein and Araujo's method. In this method an acoustic background reference medium appropriate for marine data is used which empirically remains effective in land cases. The internal multiple prediction algorithm suppresses all order of internal multiples independent of the subsurface reflectors that generate them. There are a small number of parameters whose optimum values must be chosen in an application of the internal multiple prediction. A key challenge in land data of the prediction is to choose these parameters judiciously. In this thesis we promote a stepped approach to predicting multiples in a given field data set: first, by carrying out synthetic/numerical examples; second by carrying out tests on laboratory physical modeling data; and finally by testing prediction of a field data set suspected to be strongly contaminated with internal multiples.

1.2 Objectives of the thesis

The main objective of this work is to apply 1D version of the inverse scattering series internal multiple prediction algorithm on land field data. In order to accomplish this goal, we first applied the algorithm in 1D synthetic data and then in 2D marine common offset physical model data. Finally, using these two previous experiences we applied in 2D land field data from Northeast of British Columbia, Canada.

In the first part of this thesis, we generated several simple 1D seismic models, of three primaries reflections and two interbed multiples. The specific objectives of this first experiment were: 1) evaluate the accuracy of the algorithm predicting time and amplitude of the internal multiples; 2) test how sensitive is the algorithm to certain parameters such as: source wavelet; 3) effect of the low amplitude values of the internal multiples; and 4) under or over estimation of the parameter epsilon.

In the second experiment, we acquired 2D marine common near offset physical model data and then apply the algorithm. We used this data set to: 1) evaluate how the algorithm responds to certain amounts of noise, 2) the effectiveness of the algorithm predicting multiples in 2D seismic data, 3) allowable proximity of the events, and 4) estimation of the parameter epsilon through its relation with an approximate source wavelet.

Finally, in the third part of this thesis, we applied the algorithm on 2D land field data. The specific objectives of this part were: 1) identification of internal multiples without touching the primaries reflections, 2) prove the effectiveness of the algorithm in high quality 2D field land data.

1.3 Outline of the thesis

We will present three case studies of internal multiple prediction, synthetic data, physical modeling reflection data acquired in laboratory and field data provide by Nexen. The main purpose of this work is to apply 1D version of the inverse scattering series internal

multiple prediction algorithm due to Weglein et al. (1997), and apply it to these three different cases.

First, we applied the algorithm in synthetic data in order to test the algorithm itself and evaluate how sensitive it is to some parameters, such as algorithm search limits and resolution of the data. This first case was very important as it allowed us figure out how the algorithm works and facilitated to estimating the acquisition parameters of the physical model data and to design the model itself.

As second case we applied 1D the inverse scattering internal (interbed) multiple prediction algorithm in common offset marine data over a large contrast target. This data was acquired physical model facility that University of Calgary and CREWES (Consortium for Research in Elastic Wave Exploration Seismology) possess. This provides a controlled environment to study practical algorithm issues, such as (1) choosing an optimum search parameter size, and (2) minimum proximity of sub-events. We view physical modeling environments as ideal staging grounds, within which real data from controlled targets may be analyzed to guide the choice of optimal parameters.

Land field data is the third case analyzed. The 2D land data set used was provided by Nexen. In general, land data sets present some characteristics that may make it challenging to predict internal multiples using the inverse scattering algorithm, such as noise and many temporally closely-spaced events. Nevertheless, the data used to apply the algorithm is very clean, high quality, and present strong and clear primaries, these characteristics and

our previous experience using physical model data allowed us to obtain substantial and satisfactory results.

Although the field data is 2D we decided to apply it on 1D version of the algorithm due to computationally a 2D version of this algorithm would be more complex, expensive and time consuming. We selected a group of traces of this set of data and applied the algorithm on each of them, achieving a predicted output for every trace and then compiled as whole in a stack section. Field data cases are more complex and challenging than synthetic and physical model data sets, for this reason we applied the algorithm on them in order to get a sense first how this algorithm works and how sensitive is the algorithm to the characteristics of data and algorithm parameters themselves, and also to learn what are the acceptable range of the numerical value of these parameters. Applying the algorithm on the synthetic and physical model data sets we learnt to evaluate the outputs and their credibility.

The Department of Geosciences of the University of Calgary and CREWES possess resources that made possible to test and evaluate the algorithm in different types of data, and also achieve the main and final goal of this work; application on field data, which is an important geophysical problem in both scientific academic and economic domains.

Chapter Two: Theoretical Background

2.1 Classification of seismic events

Seismic events are energy that propagates through the earth as a result of an explosion, vibration, or pressure. According to Yilmaz (1986) seismic events could be classified in two categories: primaries events and noise. Also, frequently noise is classified in coherent noise or random noise. The random noise category includes noise in the temporal direction and spatially random noise that is uncorrelated from trace to trace. The former noise usually is stronger at late times than early times in recorded data. Coherent noise includes linear noise (guided waves and ground roll), reverberations and multiples (Yilmaz, 1986).

There are also other seismic events like direct wave and ghost that fall into noise category. These two events represent portions of the wave that have not interaction with the earth. For instance, the direct wave travels through the ground straight from the source to the detectors without being reflected off or refracted by a subsurface layer**;** Figure 2.1 (left side). In presence of free-surface the direct wave may have more than one part, see Figure 2.1 (right side).

Ghosts instead are events that only exist if there is a free surface. There are three types of ghosts: source ghost, receiver ghost and source-receiver ghost. The source ghosts are waves that travel upward, reflecting at the free-surface and then ending at the receiver by propagating upward from the earth, see Figure 2.2a. Receiver ghosts are waves that start their path travelling downward from the source, then interact with free-surface and finally

end at the receiver moving downward, see Figure (2.2b). At last, the source-receiver could have attributes of both source and receiver ghosts, Figure 2.2c.

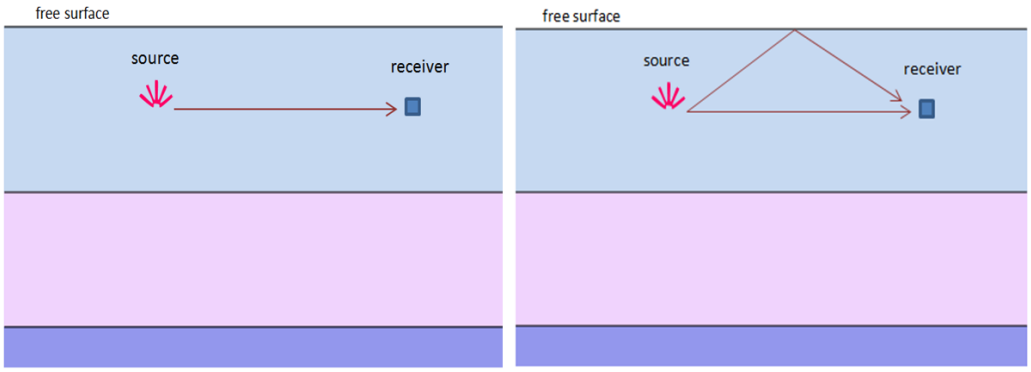

Figure 2.1: Left side: direct wave path, assuming no reflection from above. Right side: direct wave path inside of free surface layer.

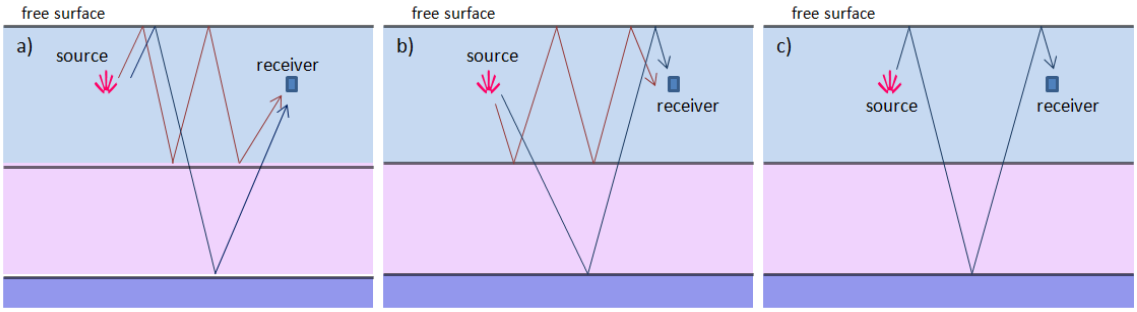

Figure 2.2: Ghosts events: a) source ghost, b) receiver ghost, and c) source-receiver ghost.

Another type of seismic event is multiples or reverberations. Most of these multiple reflections occur when there is strong impedance contrast between subsequent layers. These events have undergone more than one reflection. They are produced in the data gathering process when the signal does not follow a direct path from the source to the

geologic boundary and finally reach the receiver on the surface. Therefore, the signal arrives back at the receiver at an erroneous time.

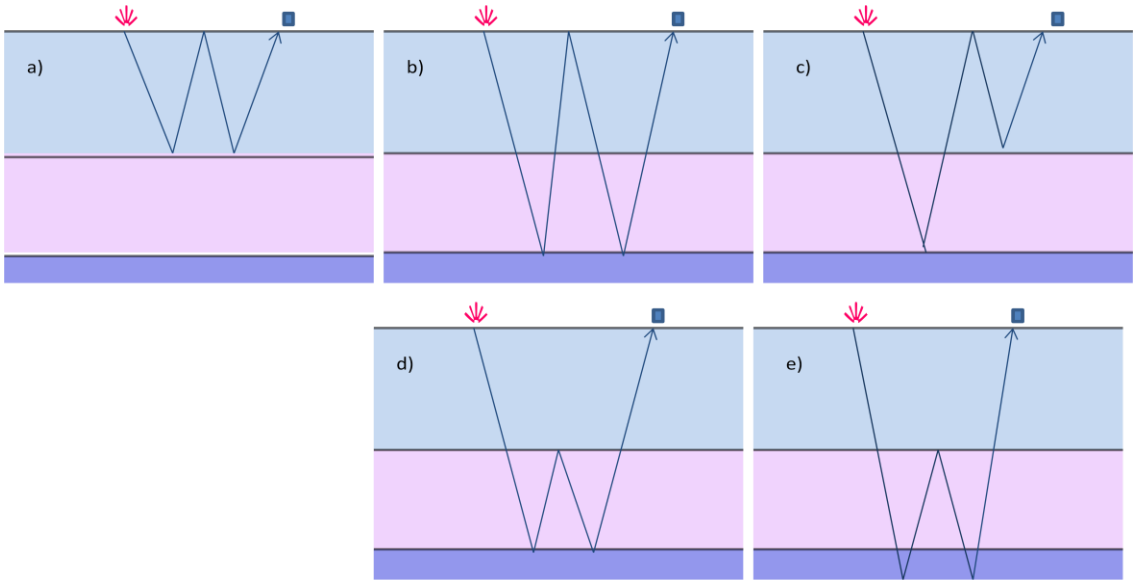

Figure 2.3: A sketch of raypaths associated with various types of multiples. The shallowest interface in each case represents the water bottom. a) water bottom multiples, b) free-surface multiples, c) peg-leg multiples, d) intrabed multiples, and e) interbed multiples. Modified from Yilmaz (1986).

We can distinguish different types of multiples: water-bottom multiples, free-surface multiples (FSM), peg-leg multiples, intrabed multiples, and interbed multiples, due to numerous configurations of raypaths associated with multiple reflections can be encountered in recorded data, see Figure 2.3, (Yilmaz, 1986). But in this work, we will differentiate multiples just in two types: free-surface multiple (FMS) and internal (or interbed) multiples (IMs).

Free-surface and internal multiples are defined as multiply reflected events that experience two or more upward reflections in the subsurface. The former consists of all multiples that

have experienced one or more reflections at the earth's surface. The latter are events that have all of their downward reflection points below the free-surface, never interact with the free-surface. Free-surface and internal multiples are classified according to their order; for example, if a FSM reflects once from the free surface is a first-order FSM (see Figure 2.4a); if reflects twice is second order (Figure2.4b) and so on. A first order internal multiple (IMs) would experiences once downward reflection (Figure 2.4c), and a second order internal multiple undergoes two downward reflections (Figure 2.4d), i.e., hits the interbed twice and so on.

2.2 1D Internal multiple prediction

The inverse scattering method attempt to identify properties of the medium from reflection data treating the problem in a series of steps or tasks: (1) removal of free-surface multiples, (2) removal of internal multiples, (3) determination of migration velocity and then migration of the primaries, and (4) inversion of these processed images to estimate changes in earth mechanical properties and density. To achieve all these, the inverse scattering method uses the following strategy: (1) recognize and disconnect the parts of the algorithm that remove or attenuate multiples events, and (2) find a direct multidimensional procedure that does not required any surface information (Weglein et al., 1997).

If these tasks are uncoupled and the two parts of the strategy are feasible, then each task of the process will be realizable without any knowledge of the subsurface. Additionally, the separation of those tasks leads to anticipate that the multiple attenuation steps will not alter primaries reflections.

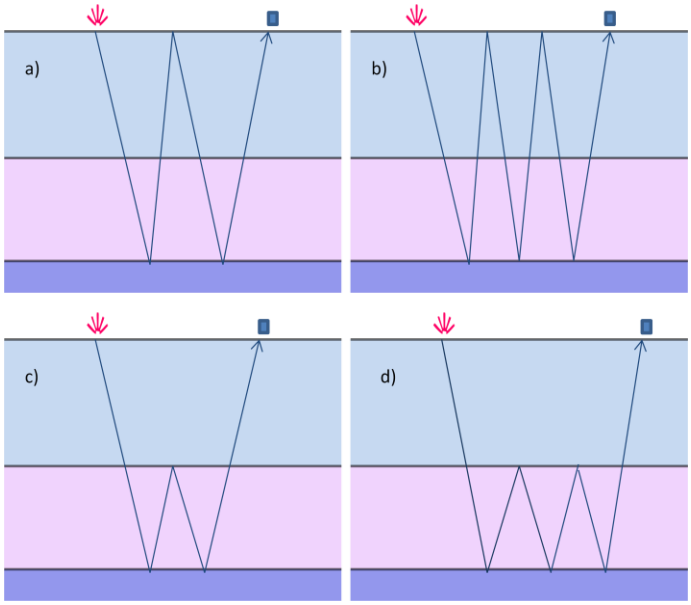

Figure 2.4: Sketch illustrating the classification of FSM and IMs: a) first order free-surface multiple, b) second order free-surface multiple, c) first order internal multiple, and d) second order internal multiples

The first term in the internal multiple attenuation series for the 1D normal incidence case is (Araujo et. al. 1994):

$$b_{3IM}(k_z) =$$

$$\int_{-\infty}^{\infty} dz'_1 \; e^{k_z i\, z'_1}\, b_1(z'_1) \int_{-\infty}^{z'_1-\epsilon} dz'_2 b_1(z'_2)\, e^{-ik_z z'_2} \int_{z'_2+\epsilon}^{\infty} dz'_3 b_1(z'_3)\, e^{ik_z z'_3} \quad (1)$$

Here k_z and z are de pseudo depth wavenumber and pseudo depth ($z=c_o t/2$) respectively. Besides, z'_1, z'_2, and z'_3 are integration variables that refers to pseudo depth positions, z'_1 and z'_3 are restricted to be larger than z'_2. The equation above predicts the travel time of the first order internal multiples and approximate their amplitude.

The parameter epsilon (ϵ) ensures that z'_1 is always greater than and not equal to z'_2 and similarly for z'_3. This parameter is related to the width of the wavelet, and could be estimated knowing the source wavelet or an approximation.

The b_1 function is the seismic data after a series of transformations. In order to obtain b_1 we begin with the measured surface data with no free-surface multiples, $D(x_g, x_s, t)$ where x_g , x_s and t are the receiver location, source location and time respectively. Then, $D(k_g, k_s, \omega)$ is obtained by performing of 3D Fourier Transform on these data. Subsequently, the data is transformed to vertical wave number, D (k_g, k_s, q_g+q_s). The third step is to transform the data to pseudo-depth establishing that $k_z = q_g+q_s$. Then, the inverse Fourier Transform is performed to the data, $b_1(k_g, k_s, k_z)$ to $b_1(k_g, k_s, z)$. Pseudo depth is an axis scaled from vertical travel time, i.e., refers to the position in space of an image obtained using a known reference velocity, reduce the computation time and cost. This conversion is often used in exploration geophysics.

Finally, the input $b_1(k_g, k_s, z)$ is used to compute the predicted multiple of equation 1. Once added to b_1, b_{3IM} suppresses all first order internal multiples. It is important to mention that this process does not remove multiples; it just attenuates them (Weglein et. al., 1998).
Equation 1 is partly intuitive and empirical and requires a deep physical and mathematical analysis to understand completely its foundations, but is clear to see that b_1 is a quantity transformed to (k_g, k_s, z) and then is broken into lower-higher-lower contributions. This latest is a key condition in the integral because allows to select the appropriate portion of

each odd terms in the series. In terms of the data this means the algorithm discriminates or locates vertically portions of the data that correspond with odds terms in the series. Algorithmically in order to select the portion of the odds terms of the inverse series and also capture the physics of Figure 2.5, the pseudo depth condition, lower-higher-lower ($z'_1 > z'_2$ and $z'_3 < z'_2$), is needed in equation 1.

Resuming, the inverse scattering attenuation method has three basics assumptions in order to work properly: knowledge of the source wavelet within the seismic frequency band, the input data must be free of surface multiple, and accomplishment of pseudo depth condition lower-higher-lower.

2.3 Subevent Interpretation

This technique does not require subsurface information to achieve the suppression of internal multiples. Moreover, the internal multiple attenuation method can be explained using the concept of subevents. This algorithm predicts an internal multiple from interpreted subevents by performing a convolution and a crosscorrelation of prestack data. For example, the first order internal multiple in Figure 2.5 is composed of three subevents that satisfy the lower-higher-lower pseudo depth condition.

To illustrate the basis of this method observe Figure 2.5. In this figure a multiple is generated at source and received at the receiver; it can be seen as the convolution and correlation of three subevents. The temporal convolution and the correlation predict the correct travel time of the multiple, and the spatial convolution predicts the proper offset,

because the sum of the offsets of two subevents minus the offset of the third will equal the offset of the multiple (Weglein et. al., 1998).

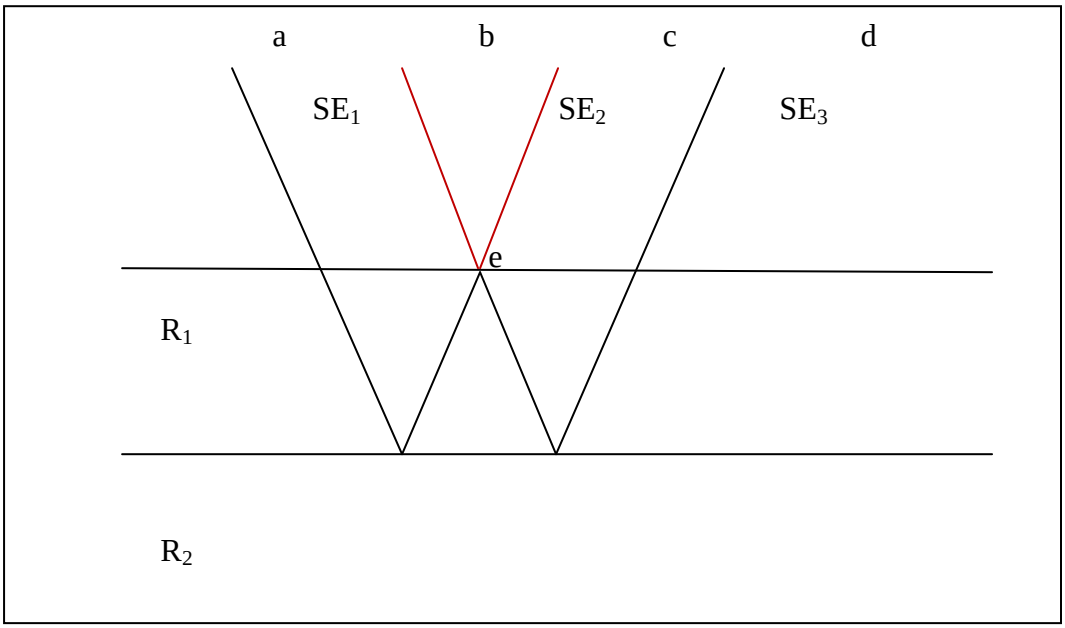

Figure 2.5: Construction of internal multiple. The first subevent which a primary reflection that travel from point *a*, reflects from the second reflector, and is measured at *c*. The second subevent is a primary that propagates from b, reflects from the first interface at *e*, and then is measured at *c*. The third subevent propagates from *b*, reflects from the second interface and is measured at *d*. (Weglein et. al., 1998).

Then, every event in the record can be thought of as a group of subevents. Convolving and correlating these subevents at particular depth the multiples are constructed. The input data to the algorithm is the multiple contaminated prestack data set. The output is a prestack data set that just contains the predicted multiples. Then by subtracting this second data set from the original input data, the multiples are attenuated or in the best case removed whilst the primaries remain undamaged (Matson, 1999).

Mathematically speaking we can describe in frequency the first subevent, a primary reflection, in Figure 2.5 as

$$SE_1(\omega) = T_1 R_2 T'_1 e^{i\omega t_2} \quad (2)$$

The second subevent, another primary, could be written in frequency as,

$$SE_2(\omega) = R_1 e^{i\omega t_1} \quad (3)$$

And the third subevent is,

$$SE_3(\omega) = T_1 R_2 T'_1 e^{i\omega t_2} \quad (4)$$

Transforming these three subevent in pseudo-depth and substituting them in equation 1 we get equation 5. Also, since the three subevents are discrete localized events and satisfy the lower-higher-lower conditions, the integration limits could be extended to ±∞.

$$b_{3IM}(k_z)$$

$$= \int_{-\infty}^{\infty} dz'_1 \; e^{k_z i\, z'_1} SE_1(z'_1). \int_{-\infty}^{\infty} dz'_2 \, SE_2(z'_2). e^{-ik_z z'_2} \int_{-\infty}^{\infty} dz'_3 SE_3(z'_3). e^{ik_z z'_3} \quad (5)$$

Applying Fourier Transform the equation below can be written in the frequency domain as:

$$b_{3IM}(\omega) = SE_1(\omega)\, SE_2(-\omega)\, SE_3(\omega) \quad (6)$$

Equation 6 describe the crosscorrelation of subevent 1 with subevent 2 followed by a convolution with subevent 3. Substituting the three subevents into equation 6 result

$$b_{3IM}(\omega) = T_1^2 R_2^2 R_1 T'^2_1 e^{i\omega\,(2t_2 - t_1)} \quad (7)$$

The actual internal multiple in the frequency domain is written as

$$IM_I(\omega) = T_1 R_2 (-R_1) R_2 T'_1 e^{i\omega (2t_2 - t_1)} \quad (8)$$

Comparing equation 7 and 8 it is noticeable that the amplitude of the predicted multiple is off by a factor of $T_1 T'_1$. For typical earth velocities this error is very small and the predicted multiple gives a satisfactory degree of attenuation. This error could be due to the fact that the leading order term in the internal multiple attenuation series does not properly take transmission effects into account and a reflection from above an interface is considered the negative of the reflection from above, (Weglein et. al., 1998).

Also, it is important to notice that the phase is correctly predicted, (Weglein et al., 1998). This algorithm predicts the proper travel time of the internal multiples based on the fact that the convolution of two arrivals will sum the travel time of those events, and the crosscorrelation will subtract their travel times. Therefore, the travel time of subevent 1 and 3 will be summed while the travel time of subevent 2 will be subtracted. In fact, the portions of the three subevents that have the same travel path will cancel.

One of the most important characteristic of this algorithm is that it selects all the subevents that suit the lower-higher-lower relation through the integration limits of the equation 1 (Weglein et. al., 1998).

Chapter Three: Internal multiple prediction using synthetic data

In this chapter we will examine using synthetic data the relationship between the parameter epsilon in the algorithm (equation 1) and aspects of the data, such as wavelet, central frequency, combination of depths and velocities, and noise. The goal is to complete this chapter with a strong intuition for optimal estimation of epsilon in order to move to physical model data and field data.

3.1 Variation of velocities

The first case consists of two primary reflectors and one internal multiple. We generated three models. The difference between them is the velocity of the second layer, and the rest of the parameters remain the same. The parameters are shown in Table 3.1. In Figure 3.1 three different models are presented and their respective input and prediction output data.

In the first model, the primary reflections are found at 0.93s and 1.3s and the internal multiple at 1.65s. See Figure 3.1 at the top. The second layer has a velocity of 3200m/s. The output prediction shows an event at 1.65s which correspond with the internal multiple present in the input data. In the second model, the velocity of the second layer is 3800m/s, therefore we find the second primary and the internal multiple sooner at 1.22s and 1.5s respectively. The output prediction presents an event at 1.5s that correspond to internal multiple.

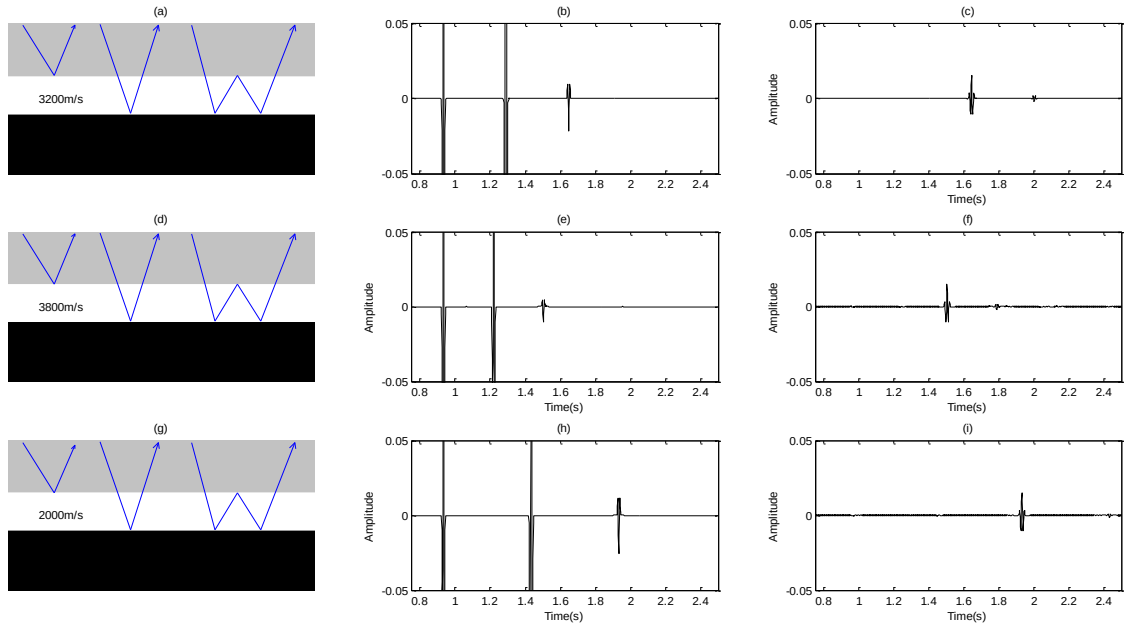

Figure 3.1: Variation of velocities of the input models and their output prediction. (a) Sketch of the input model, velocity 3200m/s. (b) Input synthetic data. (c) Output prediction. (d) Sketch of the model, velocity 3800m/s. (e) Input synthetic data of model (d). (f) Output prediction of model (d). (g) Sketch of input model, velocity 2000m/s. (h) Input synthetic data of model (g). (i) Output prediction of model.

The last model in the bottom of the Figure 3.1, shows the primaries reflections at 0.6s and 1.43s and the internal multiple at 1.93s. The velocity of the second layer is 2000m/s. In this model the algorithm predict an internal multiple at 1.93 as we expected. These three example show the accuracy of the algorithm predicting internal multiples based only in input data. The internal multiples in the three cases are predicted at the correct time with similar amplitude.

3.2 Variation of depth

In this example three models are generated, they contain two primary reflections and one internal multiple at different depths, the interval velocities remain constant between

models. The parameters are show in Table 3.2. In Figure 3.2 the models and their particular prediction are shown.

Table 3.1: Synthetic model parameters, Variation of velocities

PARAMETER	VALUE
Sample number	2048
Interval sample time	2ms
Epsilon (sample points)	14
Type of wavelet	Ricker
Wavelet central frequency	70Hz
Depth of first interface	700m
Depth of second interface	1200m
Wave speed of the source/receiver medium	1500m/s

In the first model, in the top of Figure 3.2, the primaries reflections are around 0.6 and 1.19s, and the internal multiple at 1.74s. The output prediction presents an event at 1.74s that correspond to internal multiple. In the second model, in the central part of Figure 3.2, the first layer is thinner and the second layer is thicker compare to the others model, the reflections are found at 0.4s and 1.3s and the interbed multiple at 2.25s. The output prediction for this model shows an event at 2.25 as we expected.

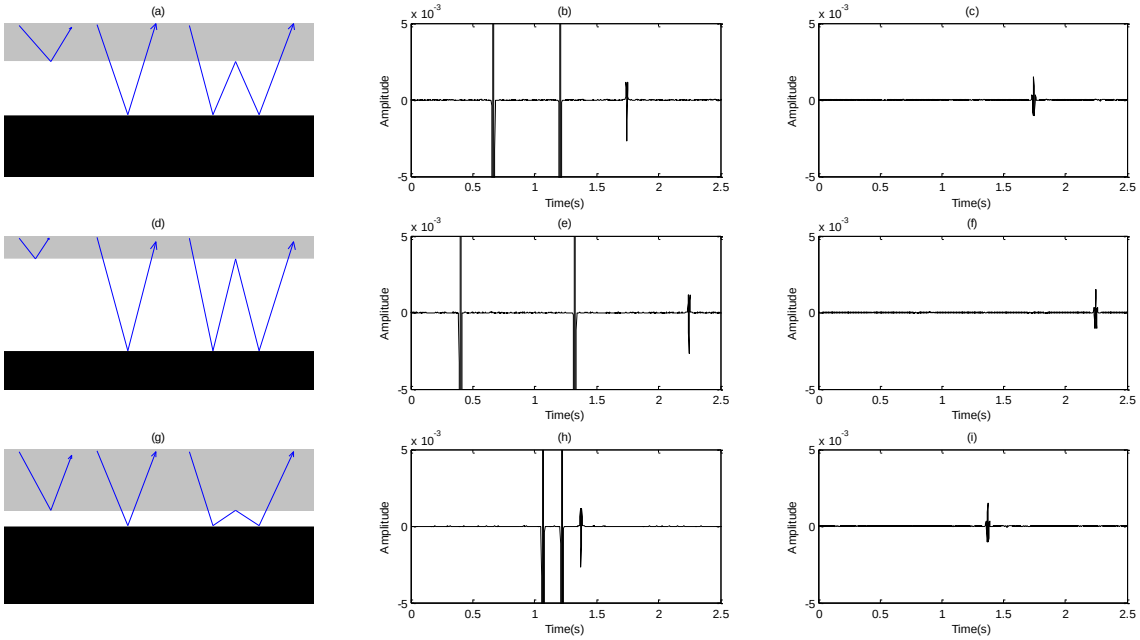

Figure 3.2: Variation of depths of the input models and their output prediction. (a) Sketch of the input model. b) Input synthetic data. (c) Output prediction. (d) Sketch of the model. (e) Input synthetic data of model (d). (f) Output prediction of model (d). (g) Sketch of input model. (h) Input synthetic data of model (g). (i) Output prediction of model.

Table 3.2: Synthetic model parameters, variation of depths in the input data.

PARAMETER	VALUE
Sample number	2048
Interval sample time	2ms
Epsilon (sample points)	14
Type of wavelet	Ricker
Wavelet central frequency	70Hz
Depths of first model	500m,1200m
Depths of second model	300m,1500m
Depths of third model	800m,1000m
Velocity first layer	1500m/s
Velocity second layer	2600m/s

Finally, the third model presents a central layer that is thinner than in the previous models, therefore the events are closer in the input data, the primaries are around at 1.06s and 1.21s and interbed multiple at 1.37s, despite in this case the events are closer the output prediction still predicts the internal multiple at the correct time and with similar amplitude. In none of these examples the output prediction damaged the primaries neither present other artifacts.

In both example 1 and 2, the source wavelet was a Ricker wavelet with a central frequency of 70Hz, and the parameter epsilon (ϵ) used was 14 sample points, which is equivalent to width of the wavelet. In these six (6) different models we used the same value of epsilon and the output prediction obtained in each case was correct.

In the next three examples examine the sensitivity of the algorithm to the parameter epsilon, with the expectation that an underestimation or overestimation of epsilon (ϵ) would lead us to a wrong prediction.

3.3 Sensitivity of Epsilon

Since the parameter epsilon is related to width of the source wavelet we made a series of tests varying the central frequency of the source wavelet in order to evaluate how sensitive the algorithm is to the parameter epsilon (ϵ). The parameters used to generate the model are given in Table 3.3.

3.3.1 High frequency data (120Hz)

We used this simple model to generate different data set with different values of the central frequency: 120, 80 and 15Hz, and applied different values of epsilon (ϵ). In the test, Figure 3.3, we used a high frequency of 120Hz to generate the data. The values of epsilon (ϵ) utilized were: 60, 15, and 8 samples points, these values correspond to data set of low, medium and high frequency. Therefore, the correct value for this particular data set is the 8 samples points; see Figure 3.3, in the bottom of right side. Even though the values of epsilon in the others two cases were wrong or optimum for different frequency value, the results obtained were correct. The algorithm predicted the internal multiple in the three cases at the correct time and similar amplitude, Figure 3.3, (d), (e) and (f). Therefore, based on these results we conclude that for high frequency synthetic data, the algorithm is capable of predict internal multiples using any a value of epsilon as long as is equal or higher than the width of the source wavelet, as we shown in Figure 3.3.

Notice that in this example the smaller value of epsilon is 8 samples points, and is the proper value according to the central frequency of the source wavelet. In the next examples we will show that is an underestimation of the value of epsilon that could lead us a wrong prediction or damaged the data, and that is the case for lower frequencies.

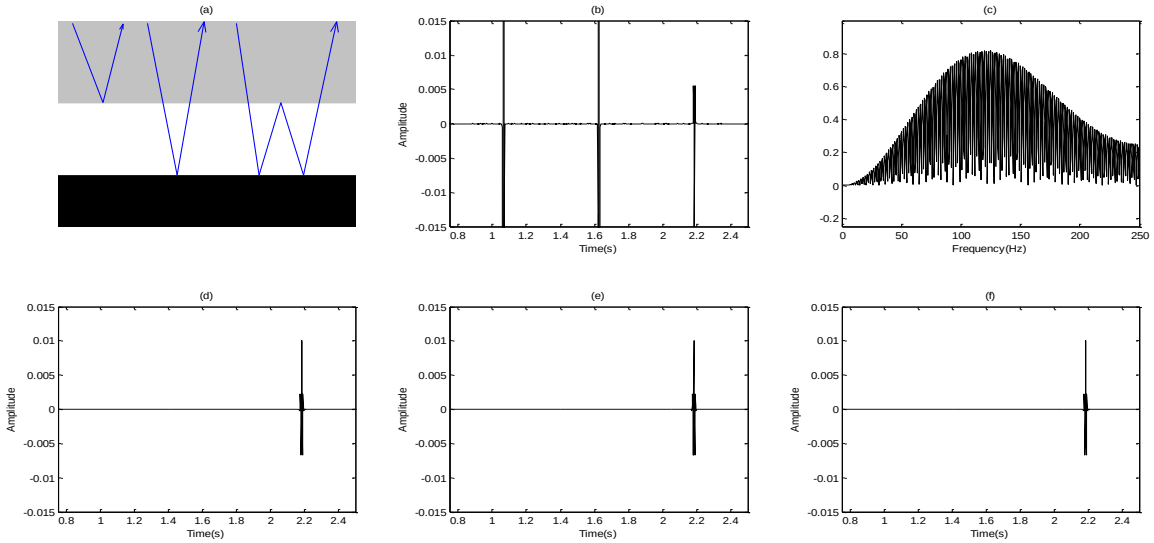

Figure 3.3: High Frequency experiment: (a) Sketch of the input model. (b) Synthetic medium frequency (80Hz) input data, two reflectors and one internal multiple. (c) Amplitude Spectrum of the synthetic data. (d) Output prediction using a value of epsilon optimum for low frequency 15 Hz (60 samples points). (e) Output prediction using a value of epsilon optimum for high frequency 80Hz (15 samples points). (f) Output prediction using a value of epsilon optimum for high frequency 120Hz (8 samples points).

3.3.2 Medium Frequency data (80Hz)

Using the parameters given in Table 3.3 we generated a synthetic data set with a central frequency of 80Hz. As the previous example the data contain two primaries reflections and an interbed multiple within, in Figure 3.4 the input data, its amplitude spectrum and the different prediction outputs are shown. In this example for a medium frequency of 80Hz we can notice how a wrong estimation of the parameter epsilon (ϵ) can lead us to a wrong prediction, for an underestimation of epsilon (smaller than width of the source wavelet) can damaged the output significantly, affecting the primaries and/or creating artifacts or wrong events. On the other hand, an extreme overestimation of the parameter epsilon would not damage the output prediction but neither shows any events, because the algorithm is not capable to identify the events.

3.3.3 Low Frequency data (15Hz)

We used the parameters listed in Table 3.3 and a central frequency of the 15Hz to generate the input data. Notice in Figure 3.5 that the wavelet is wider comparing to previous examples shown (Frequency 120Hz and 80Hz) as we expected. The proper value of epsilon for a frequency of 15Hz is 60samples points. However, different values of epsilon were tested to evaluate the results. For values of epsilon for high and medium frequency the algorithm predicted the internal multiple at the correct time but also predicted additional events that damaged the primaries. Therefore, for a low frequency data a wrong estimation, especially an underestimation of the value of epsilon would damage considerably the output prediction.

The importance of the parameter epsilon lies in the fact that events are not delta functions, they have an intrinsic form, the width of the wavelet. In chapter 2, in equation (11) we can see how the parameter epsilon was included in the equation limiting the searching of the subevents that compose the internal multiples. Without the parameter epsilon the algorithm could take one side of the wavelet as a single event and the other side as other events that obey a lower-higher-lower pseudo depth condition and construct an internal multiple, but that would be wrong because they are all part of the same event. Therefore, the parameter epsilon does not allow the algorithm to take in account these intra-events. Knowing the wavelet allow us to set in the algorithm what is the minimum width of the events can be seen as single events.

Table 3.3: Synthetic model parameters, sensitivity of epsilon.

PARAMETER	VALUE
Sample number	2048
Interval sample time	2ms
Type of wavelet	Ricker
Depths of first interface	800m
Depths of second interface	1500m
Velocity first layer	1500m/s
Velocity second layer	2500m/s

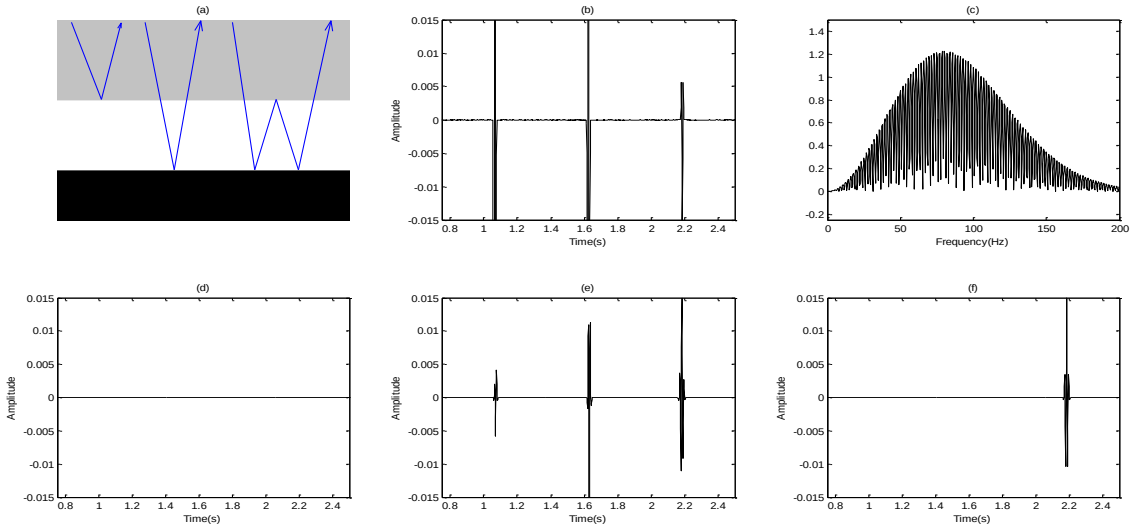

Figure 3.4: Medium Frequency experiment: (a) Sketch of the input model. (b) Synthetic high frequency (80Hz) input data, two reflectors and one internal multiple. (c) Amplitude Spectrum of the synthetic data. (d) Output prediction using a large value of epsilon, overestimation. (e) Output prediction using a small value of epsilon, underestimation. (f) Output prediction using a value of epsilon optimum for medium frequency 80Hz (15 samples points).

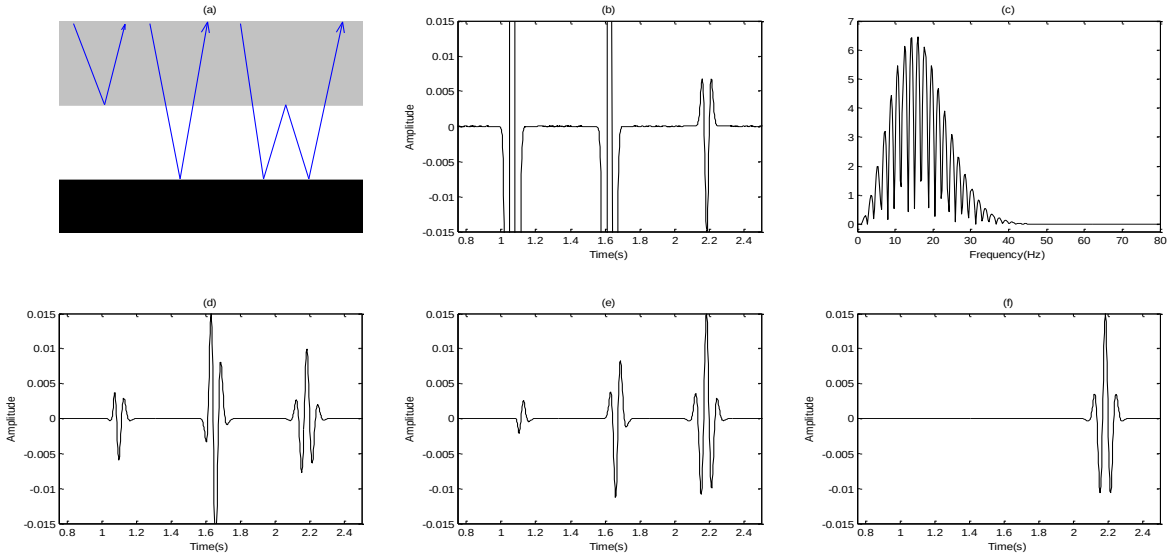

Figure 3.5: Low Frequency data (15Hz) experiment. a) Sketch of the input model. (b) Synthetic low frequency (15Hz) input data, two reflectors and one internal multiple. (c) Amplitude Spectrum of the synthetic data. (d) Output prediction using a value of epsilon optimum for high frequency. (e) Output prediction using a value of epsilon optimum for medium frequency 80Hz. (f) Output prediction using a value of epsilon optimum for low frequency 15Hz (60 samples points).

3.4 Identification of Ray paths of internal multiples

In Figure 3.6 we illustrate what ray paths correspond to particular events in the output prediction. In Table 3.4 the parameters used to construct this model are given. The first order interbed multiple that bounce in the first layer arrives at 2.06s, is clearly visible in the output prediction, at the top of Figure 3.6. The first order interbed multiple of the third interface is found at 2.26s, (middle section of Figure 3.6). The peg-leg internal multiple that hits the bottom of the first layer is shown in Figure 3.6 at bottom section, and arrives in the output prediction at 2.53s. Notice that this event was not included in the input data but still the algorithm is capable of predicts it based on the combination of subevents. Moreover, through this result we confirmed that the algorithm effectively predicts

multiples based on the combination of the events, that satisfying the lower-higher-lower condition.

Table 3.4: Parameter of the synthetic model, identification of ray paths.

PARAMETER	VALUE
Sample number	2048
Interval sample time	2ms
Epsilon (sample points)	14
Type of wavelet	Ricker
Wavelet central frequency	70Hz
Depth and velocity of first interface	500m, 1500m/s
Depth and velocity of second interface	1200m, 2000m/s
Depth and velocity of third interface	2000m, 3500m/s

3.5 Wavelet removal

In field data the source wavelet presents the effect of many components, such as source signature, recording filter, surface reflections, and receiver-array response, these components are implicit in the form of the wavelet and its frequency. In synthetic data these components are not present, but still we can remove the effect of the form and frequency of the source wavelet. The wavelet was removed from the original input data, subsequently the new input data takes the form of spikes. We tested three values of epsilon: 8, 15 and 60 samples points using the same input data. The results presented in Figure 3.7 shows that the algorithm predicted the internal multiples at the correct time and similar amplitude at any value of epsilon, which confirms that epsilon depends on the wavelet; if the data has a spike form the parameter epsilon would not be needed. Moreover, based on this result we can conclude that the response of the algorithm is not

affected for the form and/or frequency of the wavelet as long as the parameter epsilon is properly estimated. The parameters used to generate the input data are shown in Table 3.5.

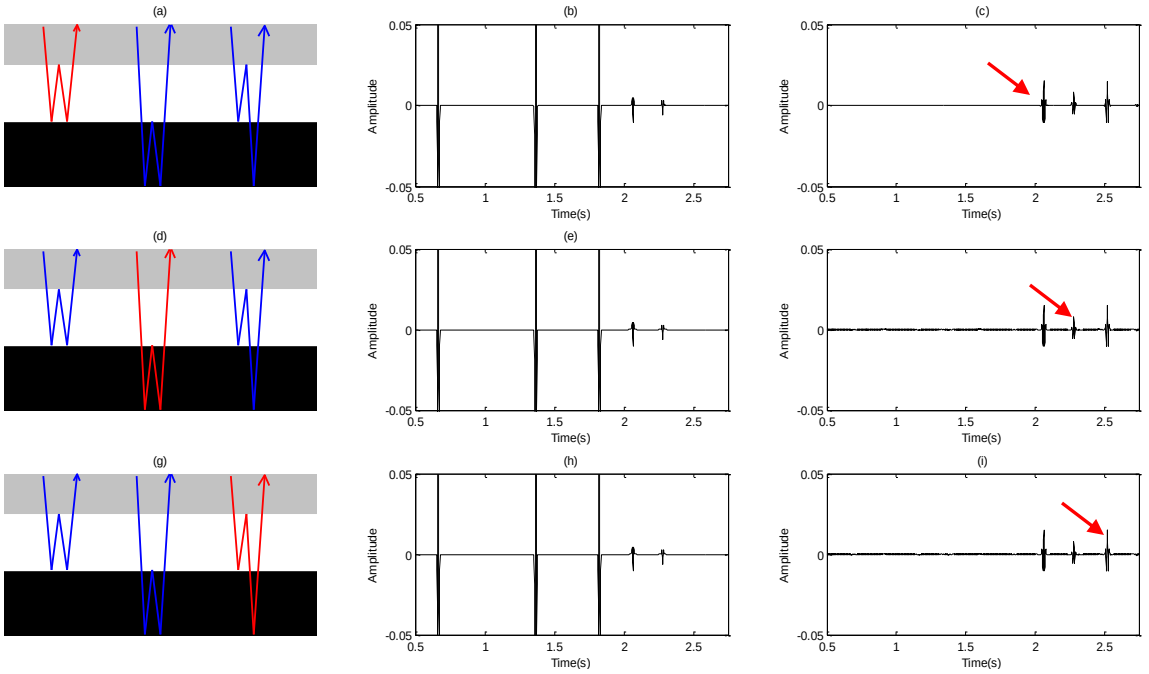

Figure 3.6: Identification of ray path of internal multiples. (a) Sketch of the model and ray paths. (b) Low Frequency input data (15Hz). (c) Output prediction, arrow indicating a first order internal multiple in the second layer. (d) Sketch of the model. (e) Synthetic low frequency (15Hz) data. (f) Output prediction, arrow indicating the arrival time of a long first order internal multiple of the third layer. (g) Sketch of the model. (h) Input data. (i) Output Prediction, arrow indicating the arrival of a peg leg internal multiple. (f) Output prediction using a value of epsilon.

In field data the source wavelet presents the effect of many components, such as source signature, recording filter, surface reflections, and receiver-array response, this components are implicit in the form of the wavelet and its frequency. In synthetic data these components are not present, but still we can remove the effect of the form and frequency of the source wavelet. The wavelet was removed from the original input data, subsequently the new input data takes the form of spikes. We tested three values of

epsilon: 8, 15 and 60 samples points using the same input data. The results presented in Figure 3.7 shows that the algorithm predicted the internal multiples at the correct time and similar amplitude at any value of epsilon, which confirms that epsilon depends on the wavelet; if the data has a spike form the parameter epsilon would not be needed. Moreover, based on this result we can conclude that the response of the algorithm is not affected for the form and/or frequency of the wavelet as long as the parameter epsilon is properly estimated. The parameters used to generate the input data are shown in Table 3.5.

Table 3.5: Parameter of the synthetic model, wavelet removal

PARAMETER	VALUE
Sample number	2048
Interval sample time	2ms
Depths of first interface	800m
Depths of second interface	1500m
Velocity first layer	1500m/s
Velocity second layer	2500m/s

3.6 Noisy data

In this experiment we generated noisy synthetic input data to evaluate how the prediction is affected for noise. The noise included in the data was statistical Gaussian noise. The model consists of two primaries and one interbed multiples. The parameters utilized to generate the model are given in Table 3.6. In the first model there is high contrast of impedance at second interface (1500m). Consequently, the respective first order interbed multiple would have high amplitude. Three frequencies were used: 30, 70, and 100Hz to generate the input data with additional noise. Appropriate epsilon values were used

according to the frequency of the input data: 60, 12, and 5 samples points. In Figure 3.8 the inputs and outputs prediction are shown. Notice that in the three cases the internal multiples cannot be differentiate from the noise, but in the outputs data the internal multiple is clearly seen.

However, the outputs predictions show a strong event at 1.75s that is the interbed multiple included in the input data. In Figure 3.9 we show the similar experiment but the model present only a variation in the velocity of the second layer; in this case the impedance contrast is less. The whole parameters are shown in Table 3.7. The amount of noise, values of frequencies and epsilon used were the same as the fore example. Notice that neither the inputs and outputs predictions show clearly the internal multiple present in the data. In this case the algorithm does not work satisfactory

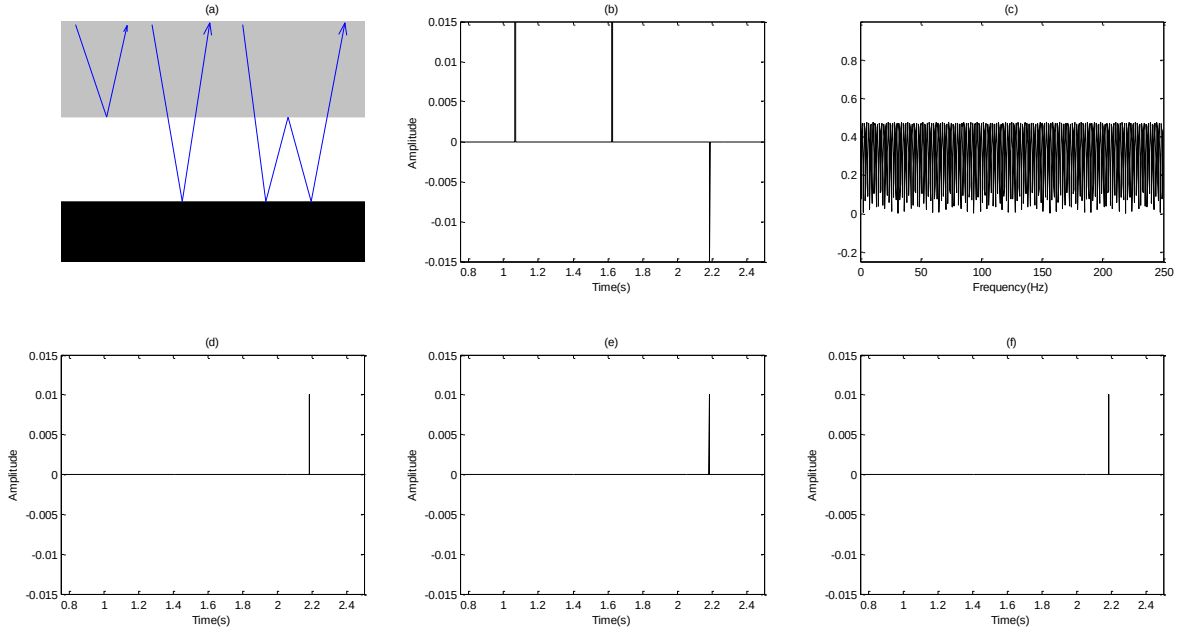

Figure 3.7: Removal of the wavelet of the input data. (a) Sketch of the model. (b) Synthetic input data, two primary reflections and one internal multiple. (c) Amplitude Spectrum. (d) Output prediction using a value of epsilon equal to 8 samples. (e) Output prediction using an epsilon of 15 samples points. (f) Output prediction using a value of epsilon of 60 samples points.

Table 3.6: Parameter of the synthetic model, wavelet removal.

PARAMETER	VALUE
Sample number	2048
Interval sample time	2ms
Type of wavelet	Ricker
Type of noise	Gaussian
Depth and velocity of first interface	800m, 1500m/s
Depth and velocity of second interface	1500m, 2600m/s

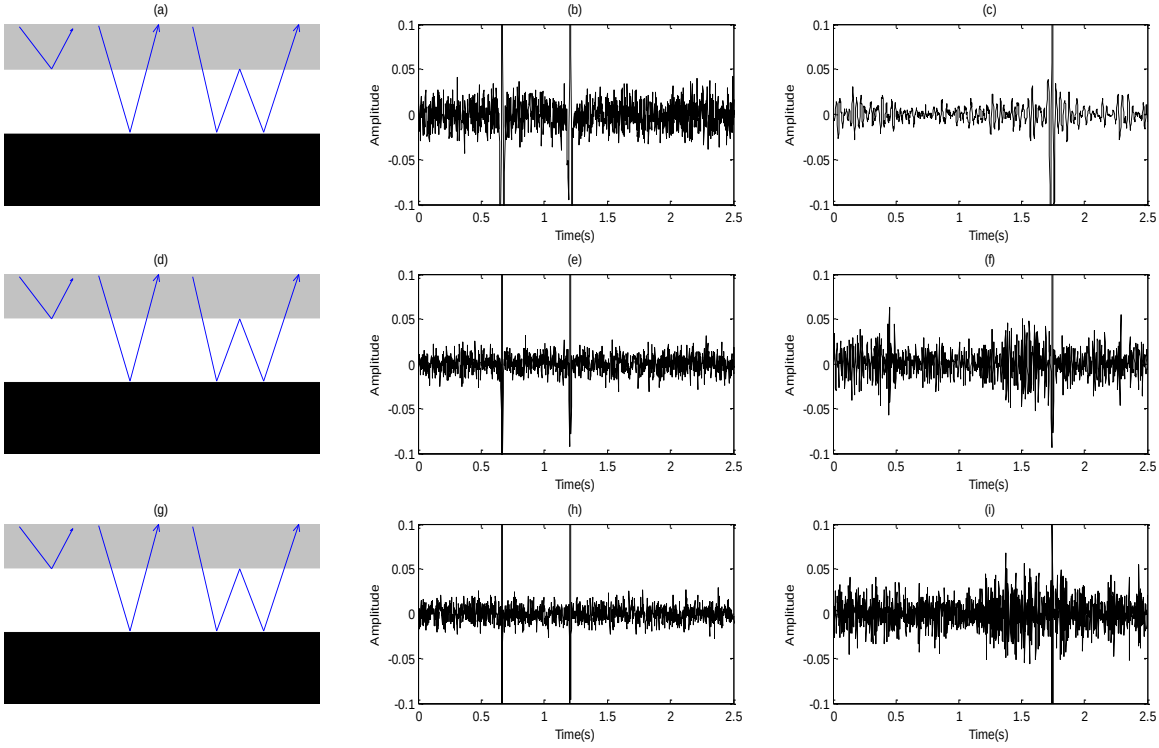

Figure 3.8: High impedance contrast model with Gaussian noise. a) Sketch of the model, b) Synthetic low frequency (30Hz) input data, c) Output prediction, epsilon 60samples points, d) Sketch of the model, e) Synthetic medium frequency (70Hz) input data, f) Output prediction, epsilon 12 samples points, g) Sketch of the model, h) Synthetic high frequency (100Hz) input data, i) Output prediction, epsilon 5 samples points.

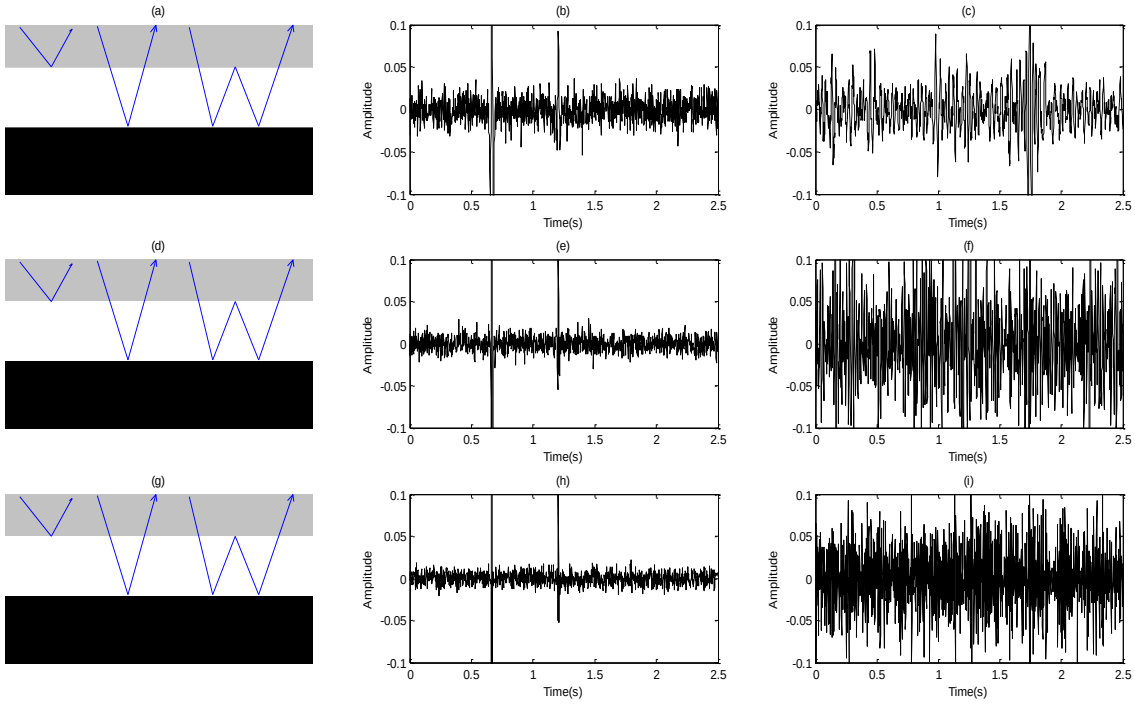

Figure 3.9: Low impedance contrast model with Gaussian noise. a) Sketch of the model, b) Synthetic low frequency (30Hz) input data, c) Output prediction, epsilon 60samples points, d) Sketch of the model, e) Synthetic medium frequency (70Hz) input data, f) Output prediction, epsilon 12 samples points, g) Sketch of the model, h) Synthetic high frequency (100Hz) input data, i) Output prediction, epsilon 5 samples points.

Based on the this results we can conclude that if the internal multiple has a strong amplitude the algorithms works correctly even though in the presence of noise, but if the internal multiple has a small amplitude and high amount of noise the results would not be accurate.

Table 3.7: Parameter of the synthetic model, noisy synthetic data.

PARAMETER	VALUE
Sample number	2048
Interval sample time	2ms
Type of wavelet	Ricker
Type of noise	Gaussian
Depths of first interface	800m
Depths of second interface	1500m
Velocity first layer	1500m/s
Velocity second layer (High Impedance contrast Model)	2600m/s
Velocity second layer (Low Impedance contrast model)	3200m/s

3.7 Summary

Based on the results found in this chapter several conclusions can be drawn:

- For different synthetic models the algorithm works satisfactory, predict multiples in the correct time and the amplitude is similar in synthetic data free of noise.
- The output prediction depends strongly on the parameter epsilon (ϵ). The importance of the parameter epsilon lies in the fact that events are not delta functions, they have an intrinsic form, the width of the wavelet.

- For smaller epsilon values, the algorithm affects the primaries. Therefore, an underestimation of epsilon could damage significantly important information present in the data. An overestimation of the value of epsilon would not damage the data, but the output will not show any internal multiples or other seismic events.
- The components of the wavelet do not affect the prediction of internal multiples using this technique as long as the parameter epsilon is well estimated.
- The algorithm works satisfactory in noisy synthetic data if there is a high contrast of impedance at the bottom reflectors that generate the internal multiple. The algorithm does not show accurate results in noisy data if the internal multiple has small amplitude.

Chapter Four: Internal multiple prediction in the lab

4.1 Physical modeling facility

CREWES and University of Calgary possess a seismic physical modeling facility that has been recently updated and improved. We used this facility to simulate a 2D marine seismic survey. The modelling facility consist of a six-axis positioning system using linear electric motors, arrays of small ultrasonic source and detector transducers, amplifiers, and signal digitization, see Figure 4.1.

The transducers convert electrical energy to mechanical energy and vice versa. The transducer that acts as a receiver is sensitive to displacement normal or tangential to the contact face, converting particle displacement to electrical signals (Mahmoudian et al., 2011). Regarding as a source, the transducer produces far field radiation patterns approximating normal and tangential displacement point (Aki and Richards, 1980). Digital data acquisition is performed by commercially available circuits boards installed in a desktop computer.

The movement of the transducers is automatically synchronized with the recording of the seismic signals. The transducers are positioned on the surface of water over an immersed solid target as if it was a marine survey (Wong et al., 2009), see Figure 4.2.

In the physical laboratory experiment a source (piezoelectric transducer) emits seismic energy into the model and the reflected wavefield is recorded. The basic assumption

supporting the physical modelling approach is that seismic waves propagate identically in both settings: scaled physical model and field scenario (Ebrom and McDonald, 1994). Physical modelling facilitates the understanding of wave propagation in elastic models and anisotropic models. Since in the physical model experiments geometries and physical properties are well known, comparison between numerical model and field data is plausible and well performed, as well as for testing of processing, imaging, and modelling algorithms (Lawton et al., 1998).

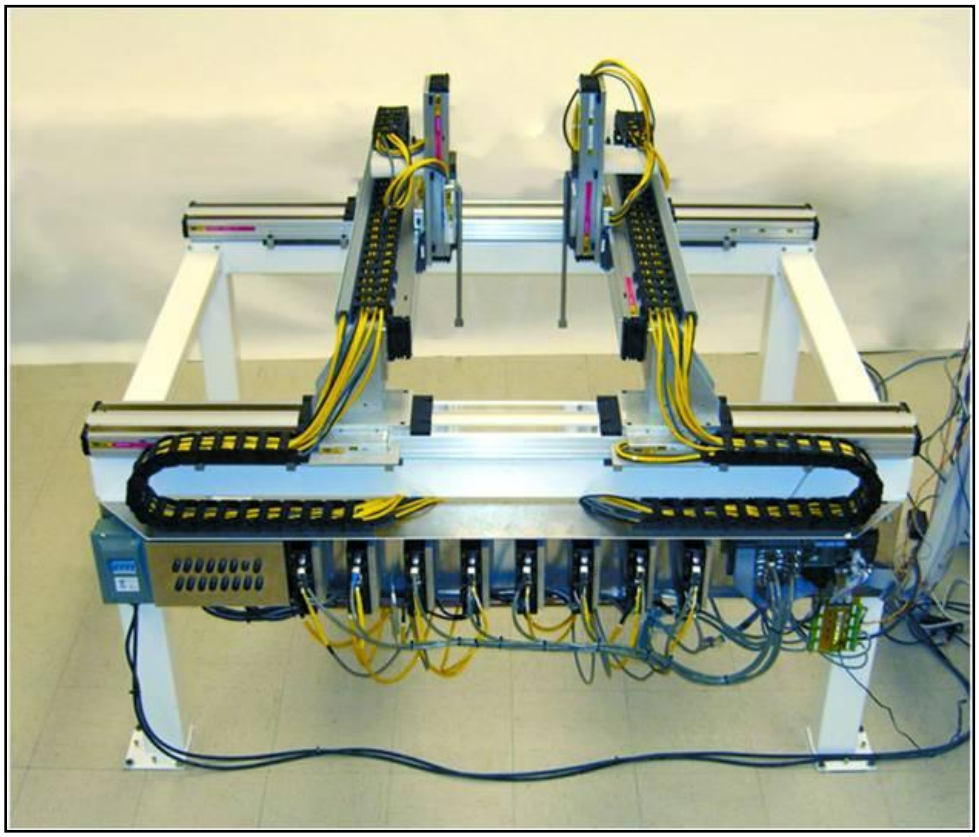

Figure 4.1: The six-axes 3D positioning system (-/+ X is left/right, -/+ Y is towards/away, -/+ Z is up/down). Modified from Wong et al. (2009).

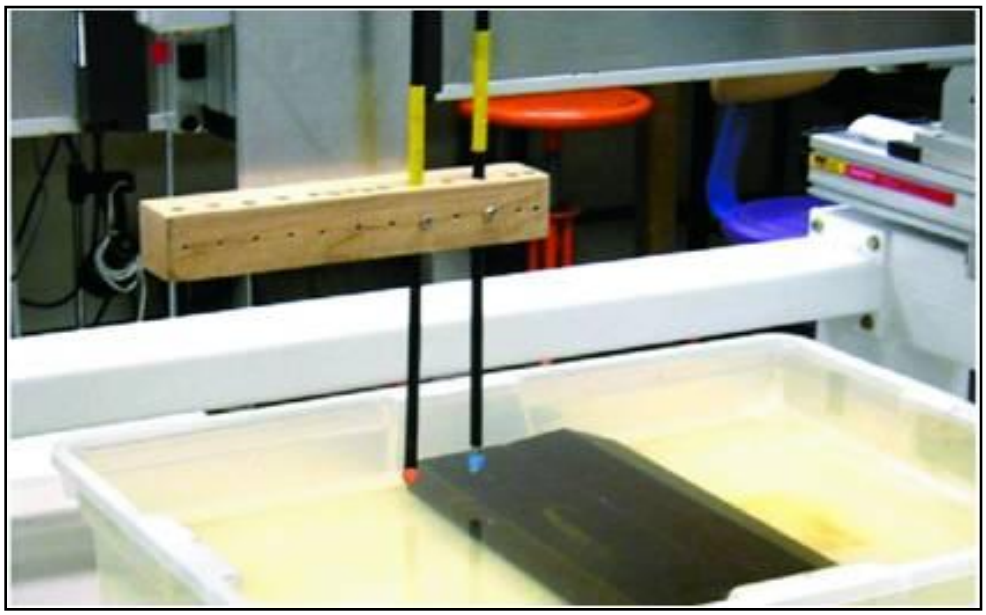

Figure 4.2: A pair of hemispheric transducers simulating a source and receiver array. Modified from Wong et al., 2009.

4.2 Model and seismic experiment

4.2.1 Model

The model used in this study consisted of a PVC slab, Plexiglass, smaller Aluminum slab, Plexiglass immerse in Water, Figure 4.3 shows sketch of this model and its physical characteristics. The scaling used for distance in the model was 1:10000, therefore, 1cm long by 2.5cm deep model represented 100m in horizontal distance and 250m in depth.

The velocities and densities of the materials in the model were not scaled. When we referred to "field scale" that represents the field dimension and the laboratory scale will be called "laboratory scaled". Using a laboratory-scale geological model Physical seismic modelling generates a seismic response (Edwards et al., 1992).

The seismic parameters used in our experiment are presented in Table 4.1.

Table 4.1: Seismic Parameters, Field Scale Dimensions.

PARAMETERS	VALUES FIELD SCALE
Receiver interval	10m
Source interval	10m
Sample time	1ms
Number of shots	400
Type of source	pulse

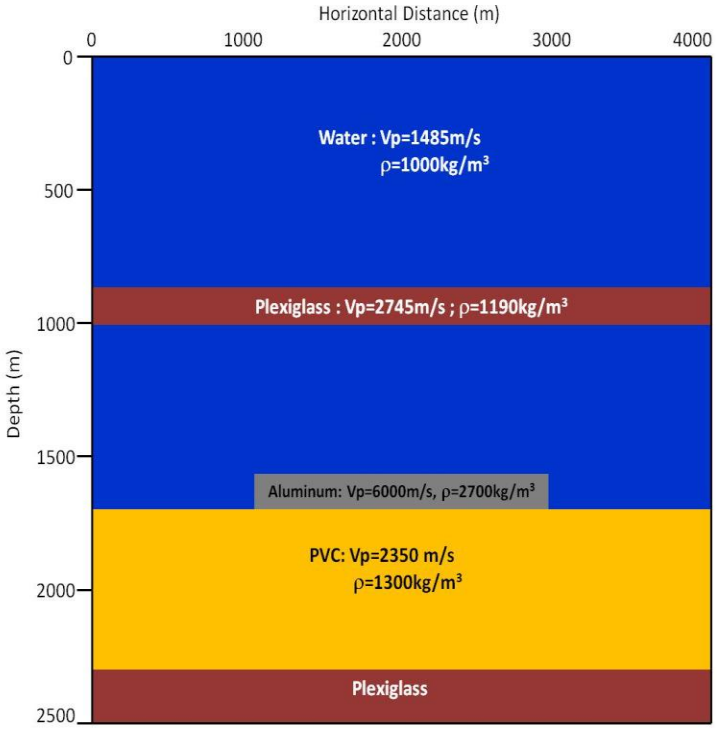

Figure 4.3: Schematic diagram of the model used.

4.2.2 Synthetic seismic model of the experimental data

As a pre-evaluation of the results of the results of this physical modelling experiment, a synthetic model was generated, convolving a Ricker wavelet with reflection coefficients. The parameters used are described in Table 4.2. Figure 4.4 shown the synthetic seismic data of this model.

Table 4.2: Parameters of synthetic model.

PARAMETER	VALUE
Sample number	4096
Interval sample time	1ms
Velocity and depth of the first interface	1485m/s at 850m
Velocity and depth of the second interface	2745m/s at 1050m
Velocity and depth of the third interface	1485m/s at 1540m
Velocity and depth of the fourth interface	6000m/s at 1685m
Velocity and depth of the fifth interface	2350m/s at 2300m
Velocity and depth of the sixth interface	2745m/s at 2500m
Epsilon	7 samples points
Type of wavelet	Ricker
Wavelet central frequency	80Hz

The input synthetic data, Figure 4.4, presents primaries reflections at 1.0s, 1.1, 1.74s, 1.79s, and 2.31s, and first order internal multiples at 1.21s, 1.84, and 2.37s. The input and output prediction are shown in Figure 4.6. Notice in this figure that the output prediction is not affecting the primary reflections present in the input data. The algorithm predicted first order internal multiples around 1.21s, 1.84s, and 2.37, Figure 4.5. There is ringing effect or reverberations noticeable in the output prediction section. The energy is trapped in the water and aluminum layers, between 1000 to 1700m; this area is bound by strong reflecting interfaces. Each rebound generates successive multiples arrivals. The internal multiples that arrive at 1.8s and 2.3s present strong amplitude due to the high reflection coefficient of the water and aluminum interfaces. The combination of these materials is an excellent multiple-generating medium.

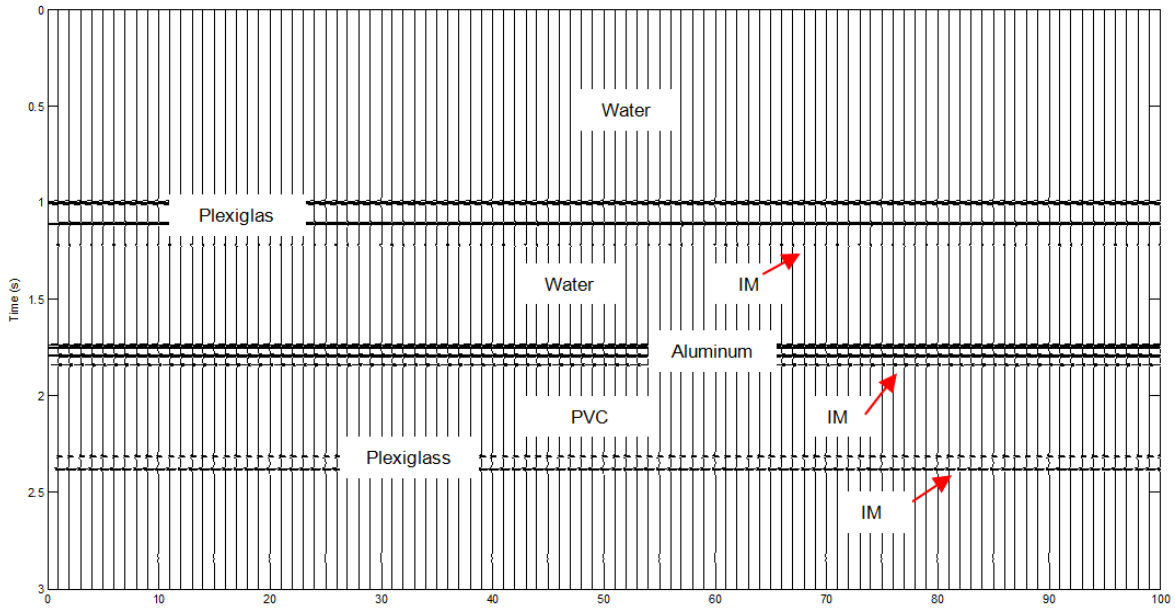

Figure 4.4: Synthetic input data of the physical model experiment.

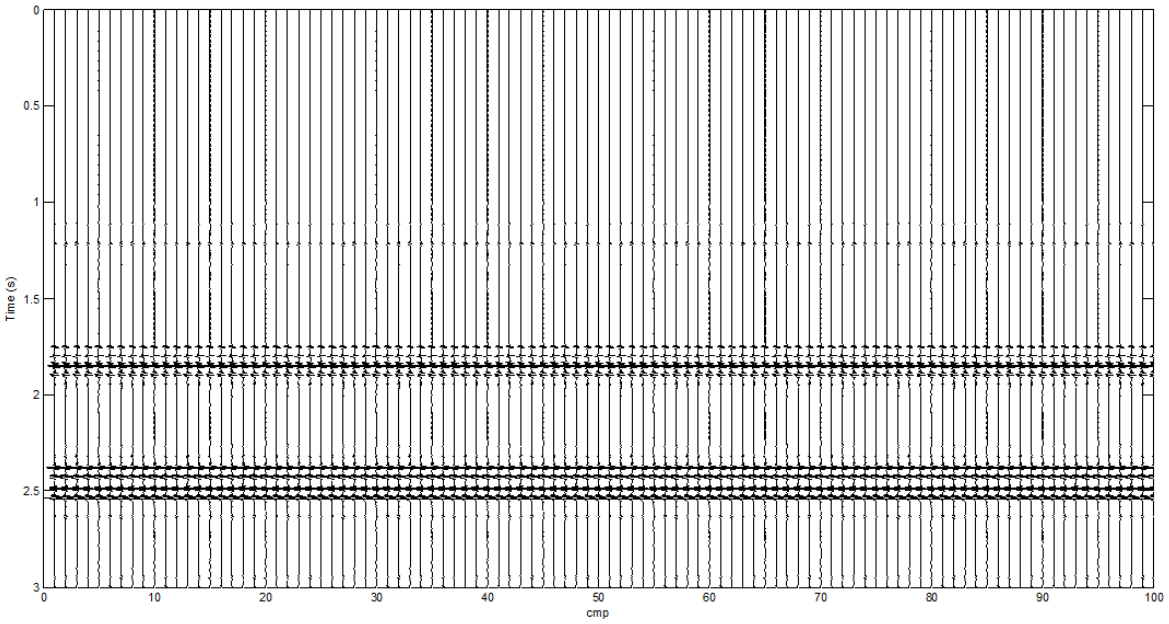

Figure 4.5: Output prediction of the synthetic model of the physical model experiment. The section only contains internal multiples.

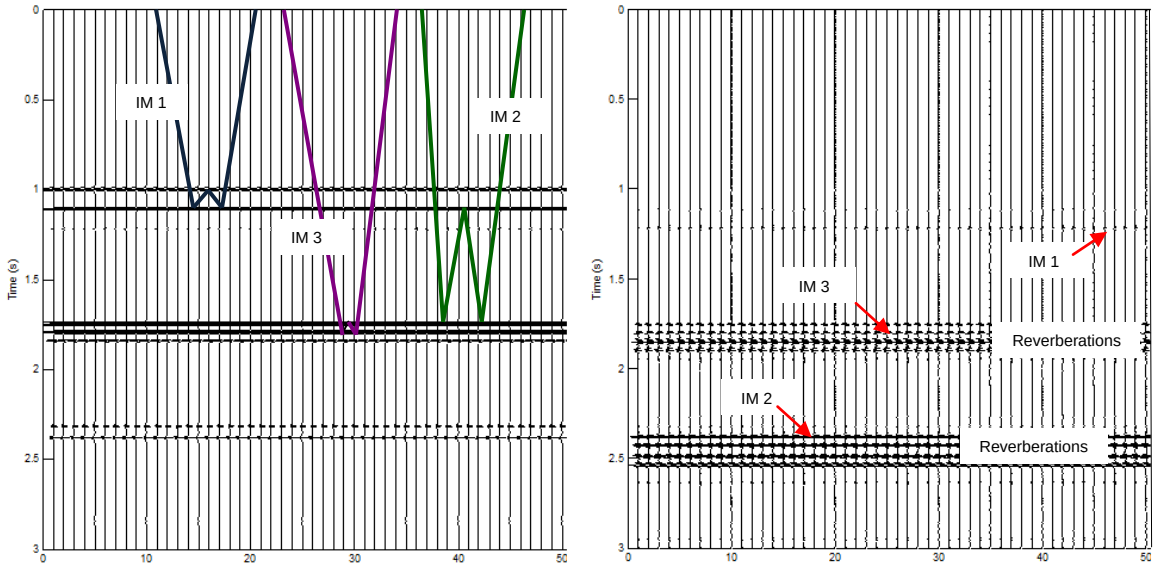

Figure 4.6: Left side: Input synthetic data of the physical model. Right side: Output prediction of the synthetic model.

4.2.3 Seismic Experiment

We conducted a 2D common-offset seismic survey over the model shown in Figure 4.3, with 401 traces at a spacing of 10m (field scale). The source and the receiver were slightly immersed in the water. The frequencies emitted varying between 5 to 100Hz (field scaled) (Hrabi, 1994).

The main objective of the utilization of physical model was to obtain high quality low noise seismic data, with clear and strong primaries and, internal multiples in order to test internal multiple attenuation algorithm.

4.3 Data processing of the physical modeling data

The raw data is shown in Figure 4.7. The figure shows a common offset stack of all data recorded. The processing flow implemented for this data set is listed in Table 4.3. The dominant frequency is 35Hz. The data in general is high quality, not noisy and the reflections are well defined in the entire section. Figure 4.8 shows the seismic data set after processing. This data set is the input of the algorithm.

Table 4.3: Processing work flow.

STANDARD FLOW
Deconvolution
Velocity analysis
Statics (No surface consistent)
Noise Attenuation filter

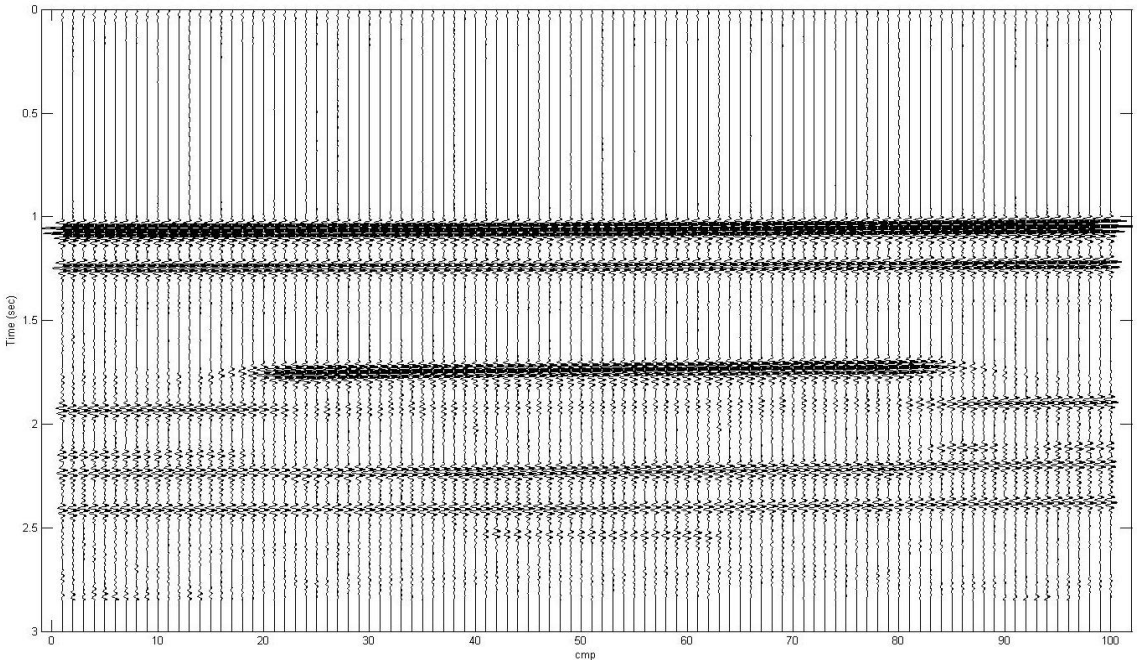

Figure 4.7: Common- offset section: raw data

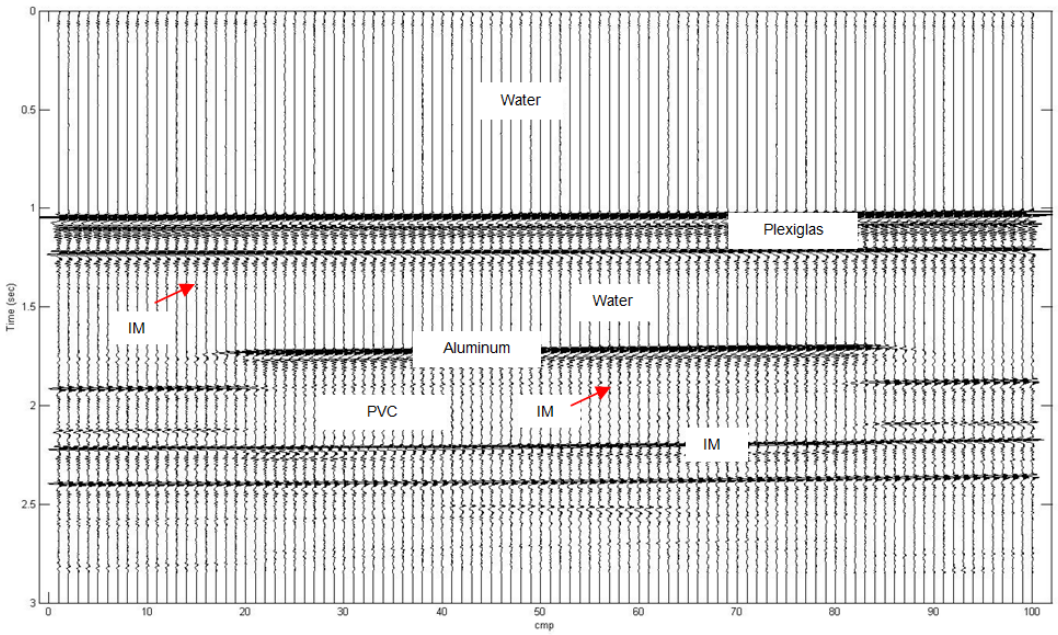

Figure 4.8: Common-offset section: after processing

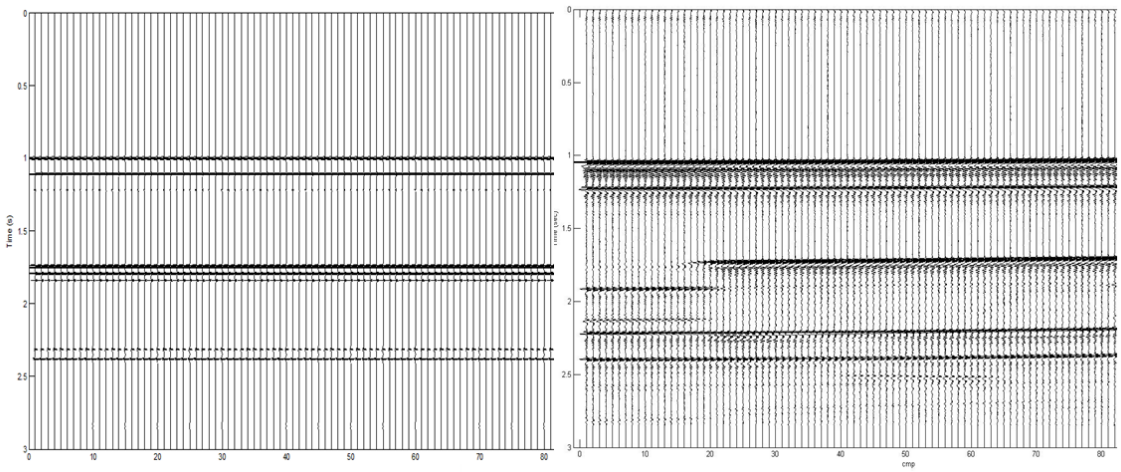

Figure 4.9: Comparison of the input synthetic data (left side) and input physical model data (right side).

4.4 Estimation of epsilon

Crosscorrelation is a measurement of the similarity or time alignment of two signals, usually applies in the time domain. The phases of these two signals are subtracted, and maximum correlation occurs at zero lag. The autocorrelation is the correlation of a signal with itself; it is the similarity between observations as a function of the time separation between them. Autocorrelation is a very useful mathematical tool for finding repeating patterns, such as the existence of a periodic signal which has been buried under noise, and/or identifying the missing fundamental frequency in a signal implied by its harmonic frequencies. Autocorrelation is frequently used in seismic processing to designing the deconvolution operator. In this work, the autocorrelation is used to estimate the source wavelet in subsequently a value of parameter epsilon (ϵ). Figure 4.10 shows the autocorrelation of input data.

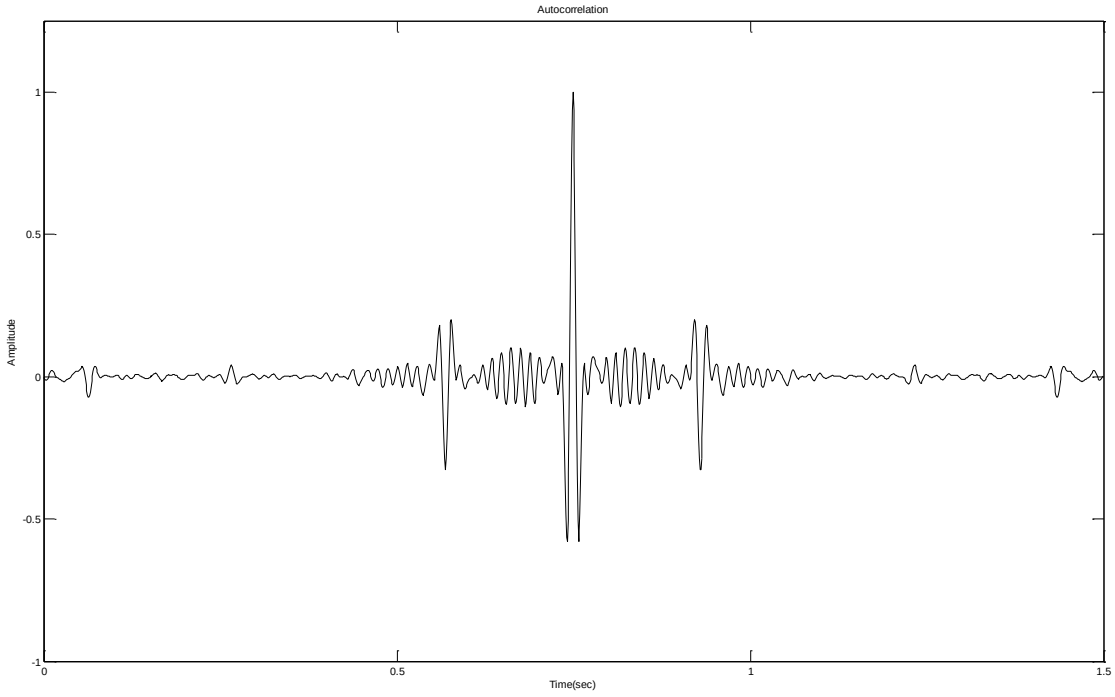

Figure 4.10: Autocorrelation of the physical model data

4.5 Application of the algorithm on physical model data

We applied our 1D multiple attenuation algorithm on physical model data and the results are quite satisfactory. Figure 4.9 shown a comparison between the input synthetic data and the input physical model data, the models are very similar; however present a slight difference in the arrival times. The prediction is showen in Figure 4.11. Setting at epsilon (ϵ) value of 50 (sample points) we predicted internal multiples reflections at 1.4, 1.9, 2.3 2.6 and 2.7 seconds as we expected according to the model. The form of the wavelet is affecting the output prediction. Notice in Figure 4.11 that the output prediction does not affect primaries reflections.

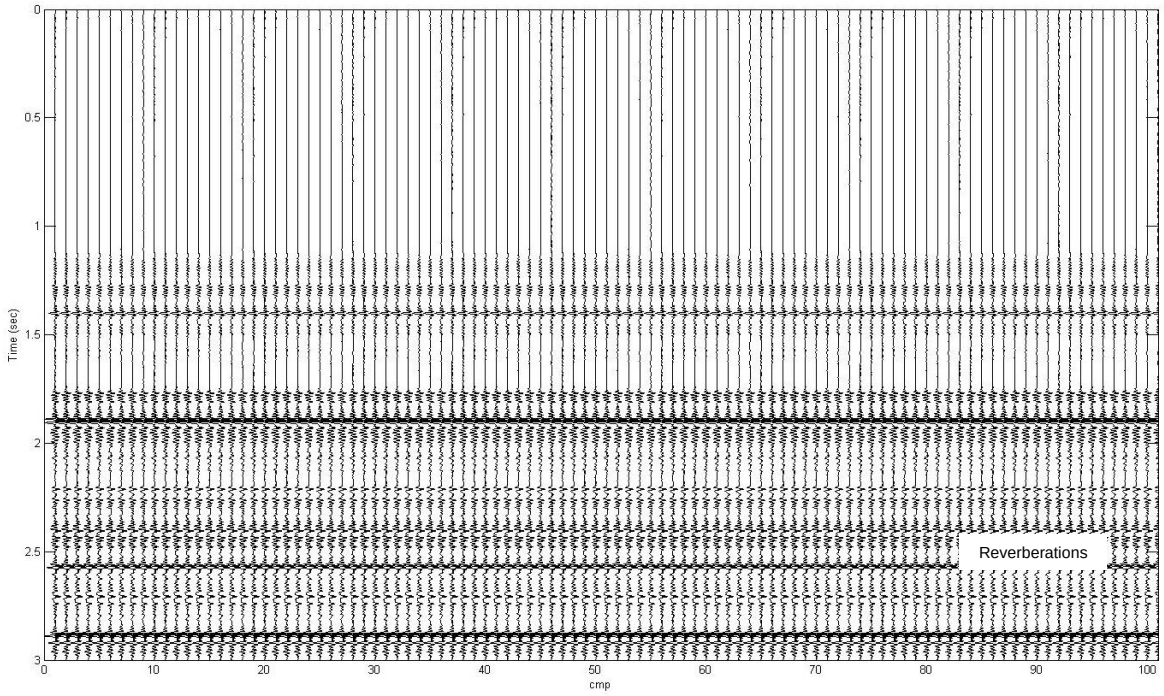

Figure 4.11: Common- offset section: Output prediction

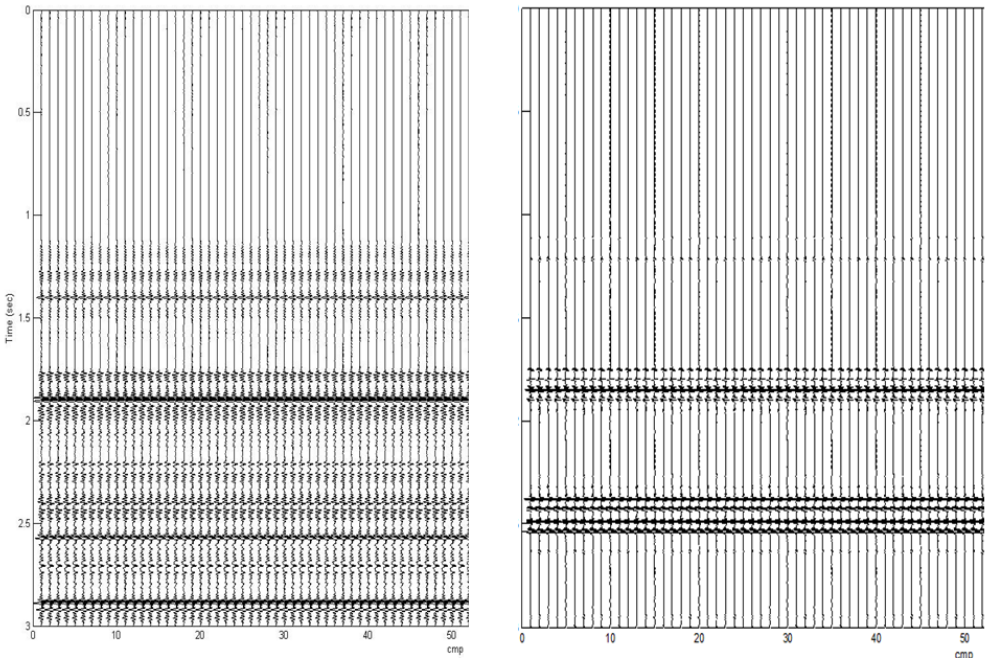

Figure 4.12: Comparison between output prediction data of the physical model (left) and output prediction (right) of the synthetic model.

In Figure 4.12 a comparison between the output prediction of synthetic model and the output prediction is given, the models present the same events with a slight shift in time, however the pattern is very similar, both output predictions present reverberations or ringing effect. A certain amount of seismic energy is not been transmitted from one layer to the next through the water and aluminium layers. It remains trapped within of these layers producing additional arrivals on the section at each rebound. Figure 4.13 shows a comparison between input data and output prediction; observe in this Figure the arrival of the internal multiples at the correct time and similar amplitude. Notice in Figure 4.13 that the strongest internal multiples is IM3 due to the high contrast of impedance between the aluminum layer and water, is very strong in the input data and output prediction.

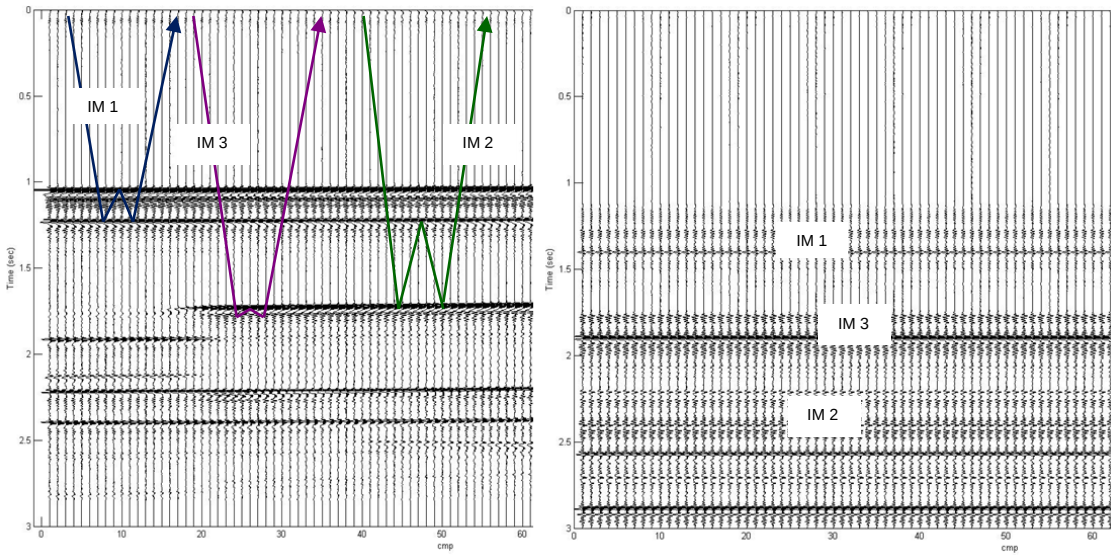

Figure 4.13: Comparison of input data and output prediction of the lab data, physical model

4.6 Summary

In this chapter we described the design and acquisition of a laboratory data set, and the use this data as an input for the internal multiple attenuation algorithm works in physical model data. We conducted a 2D common offset seismic survey in physical model lab of the University of Calgary. Pre-processing (e.g. statics, velocity analysis, deconvolution, filtering) of the data was required. The physical modeling study confirms the conclusions of the synthetic analysis, in particular motivating the development of a method for estimation of optimum epsilon (ϵ) via autocorrelation of the input data. The ability to confirm the presence of multiples, suspected to be present from a ray path analysis in the laboratory model with known elastic properties, suggests field data, especially in the presence of wells logs may be a similar analysis.

Chapter Five: Internal multiple prediction on land seismic data

For the exploration of oil and gas reservoirs, multiples can be one of the main issues in applying the seismic method. In this chapter we will present the methodology and results of the application of the algorithm on land field data. Two experiments will be explained: 1) synthetic data test, using well log information (velocity and density logs), and 2) field data test, performed on 2D land seismic data. Both data sets were donated by Nexen Inc., and belong to the northeastern of British Columbia (NEBC). Although both data sets are in the same area, the well does not intercept the 2D seismic line; in fact this well is 5km away from the seismic line. For this reason, we excluded some geological intervals of the synthetic model that are present in the well log information but not in the seismic line, such as: Bucking Horse, Spirit River, Tetcho, Muskwa and Evie, in order to compare the well markers with major seismic reflections and their corresponding internal multiples.

5.1 Geological Background of the major reflectors

The 2D line used in this work was acquired in northeast of British Columbia (NEBC). The surface of the area is mostly tills rich in clay and sediments of origin glaciolacustrine. The area presents in some places thick organic deposits in poorly drained areas (Levson et. al. 2005). In the next sections, we will describe briefly the geological characteristics of the formations that are present in the 2D seismic line, see Figure 5.1, these formations are named: Banff, Exshaw, Jean Marie and Otter Park. Moreover, well log information of the area was available and used for identification of which surfaces were generating internal

multiples due to high contrast of impedance and also for the construction of the synthetic model of the area.

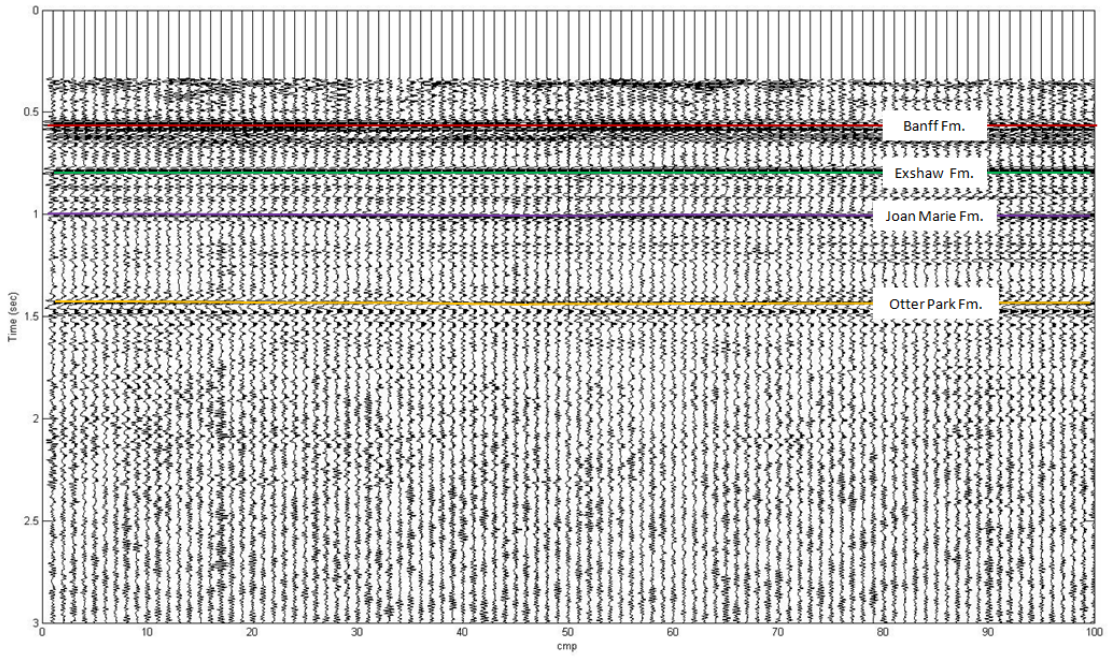

Figure 5.1: 2D seismic section illustrating the tops of the major geological markers: Stack section with multiples, after processing, input data.

5.1.1 Banff Formation

The Banff Formation belongs to the Fort St Jonh Group (Lower to Mid Cretaceous), in particular Banff Formation is the age Mississipian. This formation consist of shales and marlstones, bedded chert and carbonates towards the east and the surface. The thickness of the formation in this area is around 140m. The Fort St. John Group was deposited in a marine environment. The shallower part of this formation is a sequence of interbedded sandstones, siltstones, and shales (Glass, 1997). In the well log, Figure 5.2, the Banff formation exhibits high frequency variations in velocity and density logs. In the seismic section, Figure 5.2, this reflector is found around 0.52s.

5.1.2 Exshaw Formation

The Exshaw Formation consists of black shale in the lower part, and siltstone and limestone in the upper part. It has a thickness of 45 metres approximately. Its age is Mississipian as well. The Exshaw Formation is unconformably overlain by the Banff Formation. In the well log there is an abrupt increment of the velocity (~5550 m/s) that start at the top of the formation that also corresponds to low values in the GR. The density log is quite uniform; values are around 2700kg/m^3, except for two picks at 820 and 860m (TVD) of unknown genesis, Figure 5.2.

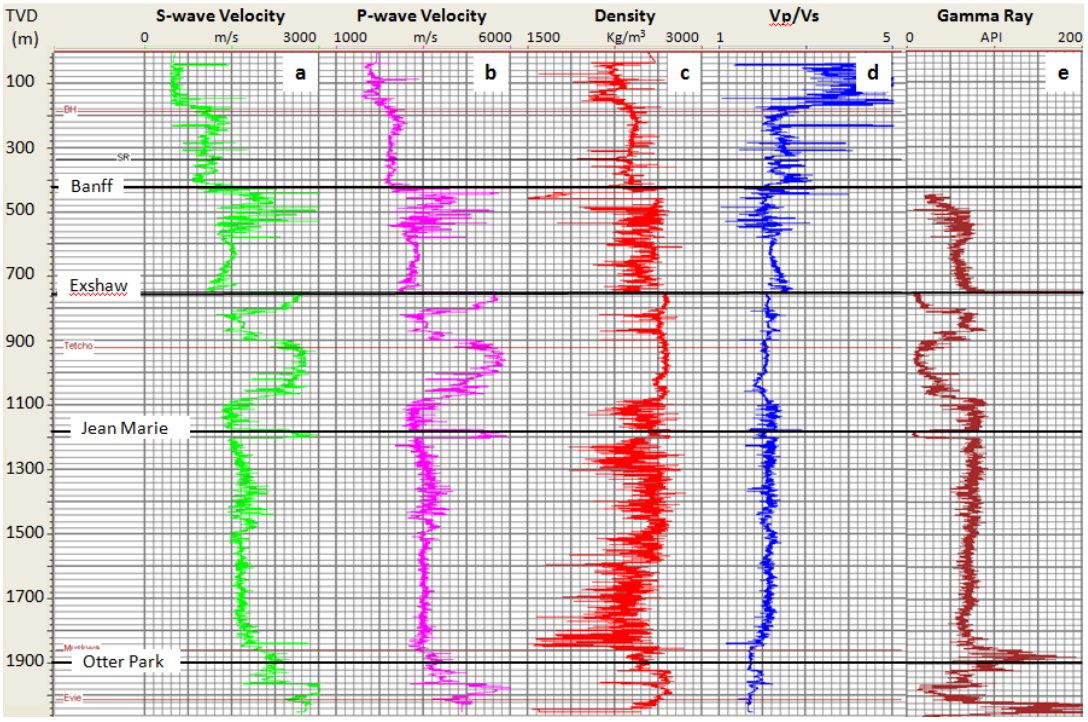

Figure 5.2: Well log from the area: a) S-wave velocity log, b) P-wave velocity log, c) Density log, d) Vp/Vs, e) Gamma Ray. Modified from Zuleta (2012).

5.1.3 Jean Marie Formation

The Jean Marie Formation is a member of The Redknife Formation of Frasnian age (Upper Devonian), is composed of argillaceous, silty and dolomitic fossiliferous limestone. The P-wave shows a strong velocity pick of 5250m/s in the interface Exshaw-Jean Marie, but rapidly changes to a uniform tendency with an average velocity of 3450m/s. This formation exhibits high frequency variations in density, Figure 5.2.

5.1.4 Otter Formation

The Otter Park Formation is composed by medium to dark grey calcareous shale of Givetian age (Middle Devonian). This formation also present radioactive siliceous black shale beds (McPhail et al., 2008; BC Ministry of Energy and Mines, 2011). This shale has a thickness of 270m towards the southeast of the Horn River Basin and thins to the north and west. This formation was originated from deposits of clays, fine siliceous (silica-rich) muds, and organic matter, in the deeper, poorly oxygenated waters. Otter Park has increase of velocity in the P-wave log and a decrease Gamma Ray in the deeper part of the formation due to the presence of organic lean argillaceous carbonates, see Figure 5.2.

According to geological information and well logs we expected a high impedance contrast between the source-receiver medium and Banff Formation, and Jean Marie and Otter Park reflectors because a high velocity values. These high impedance contrasts can potentially causes the generation of internal multiples bouncing between these reflectors or the combination of them.

Table 5.1: Parameter used to generate the synthetic model of the NEBC.

PARAMETER	VALUE
Sample number	2048
Interval sample time	2ms
Velocity and depth of the first interface	3140m/s at 420m
Velocity and depth of the first interface	3900m/s at 750m
Velocity and depth of the third interface	3450m/ s at 1180m
Velocity and depth of the fourth interface	5250m/s at 1900m
Epsilon	13
Type of wavelet	Ricker
Wavelet central frequency	80Hz
Wave speed of the source/receiver medium	1500m/s

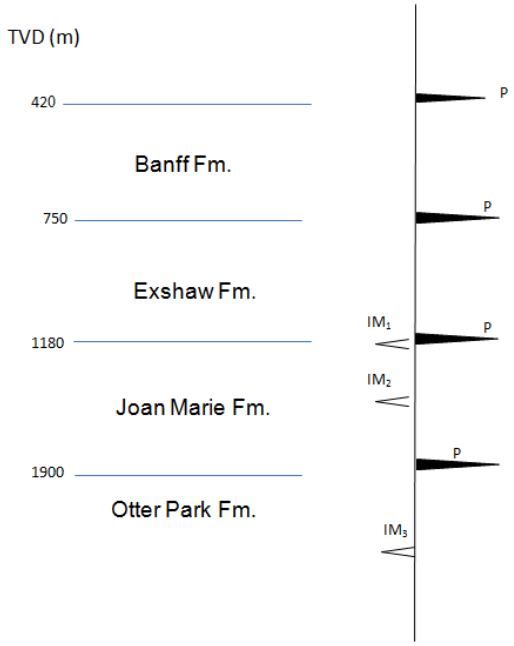

Figure 5.3: Sketch of the synthetic model of the area.

5.2 Synthetic data test

Well log information of the area is shown in Figure 5.2. This information allowed us to generate a synthetic seismogram, convolving the reflectivity obtained from well logs with a Ricker wavelet. The well log information represents a regional scenario of the area.

The main objective in generating a synthetic seismogram using well log information is to predict the seismic response of the area, and to evaluate how the algorithm works in this geological setting, and predict internal multiples based on the combination of subevents, only considering primaries, and then compare the results of the field data in terms of time and amplitudes. We also used this model to pre-evaluate the value of the parameter epsilon (ϵ), and use it as reference in the field data test.

In order to simplify the synthetic model the following formations were excluded: BuckingHorse, Spirit Horse, Tetcho, Muskwa and Evie. Figure 5.3 presents a sketch of the synthetic model of the area. This illustration shows the principal first order internal multiples (IM) that can be constructed based on the combination of the main primaries (P) known. Details of the parameter used for the synthetic model are show in Table 5.1.

Figure 5.4 shows the input synthetic data, this section contain four primary reflections at 0.56s (Banff), 0.77s (Exshaw), 1.0s (Jean Marie), and 1.41s (Otter Park), and three first orders internal multiples around 1.0, 1.21s, and 1.83s. The output prediction is shown in Figure 5.5, in this figure internal multiples are found at 1.0s, 1.2s, 1.4s, 1.65s, 1.83s, 2.0s and 2.3s The value of epsilon (ϵ) used was 13 sample points.

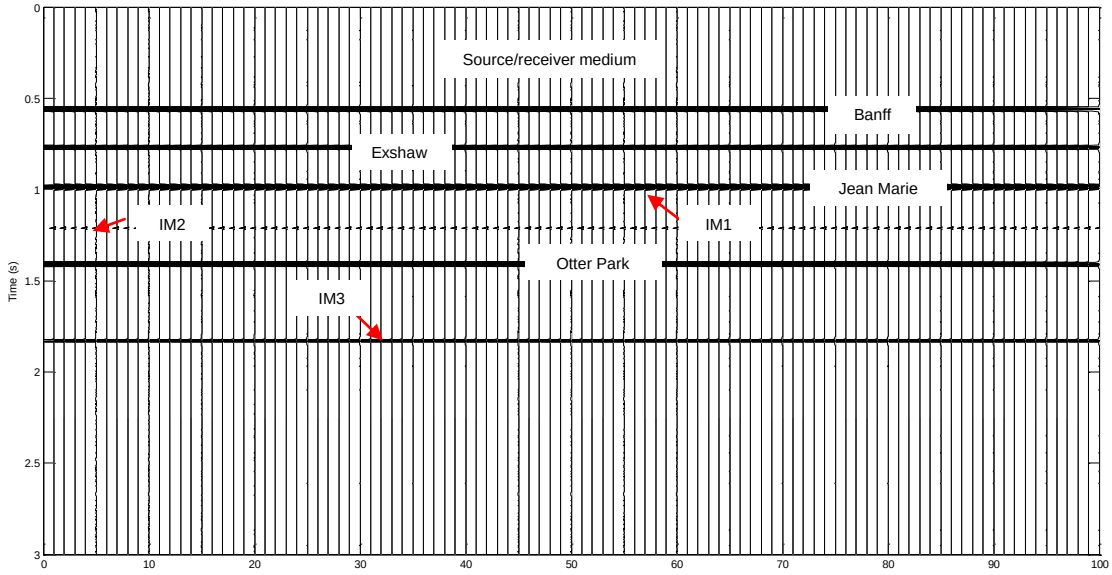

Figure 5.4:Synthetic input data based on well log information. Four primaries reflections (Banff, Exshaw, Jean Marie and Otter Park) and three internal multiples (IM)

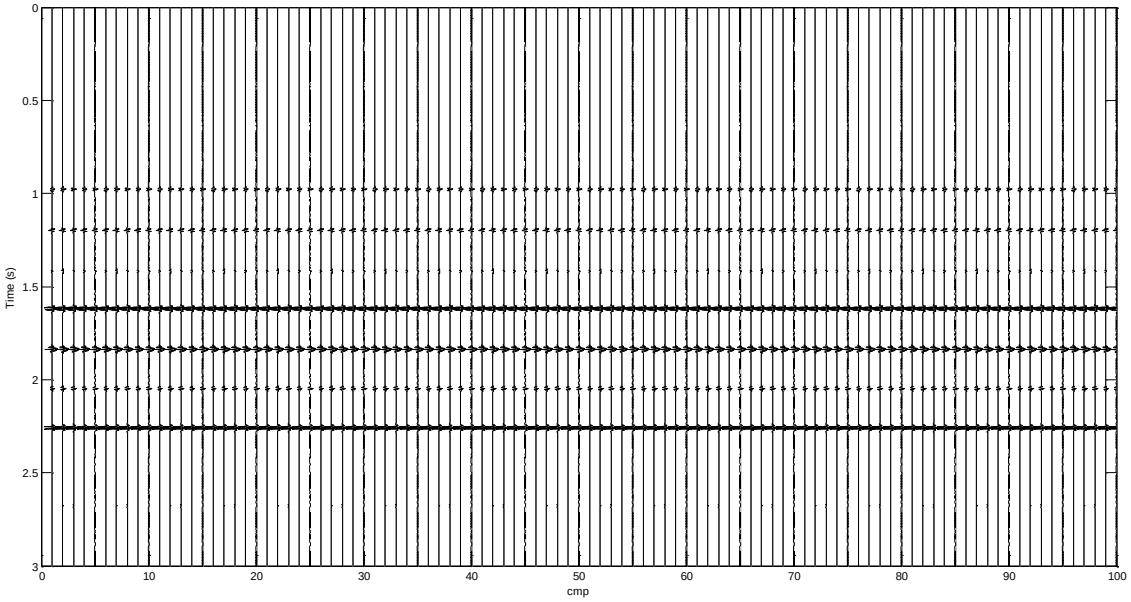

Figure 5.5: Output prediction, only contain internal multiples.

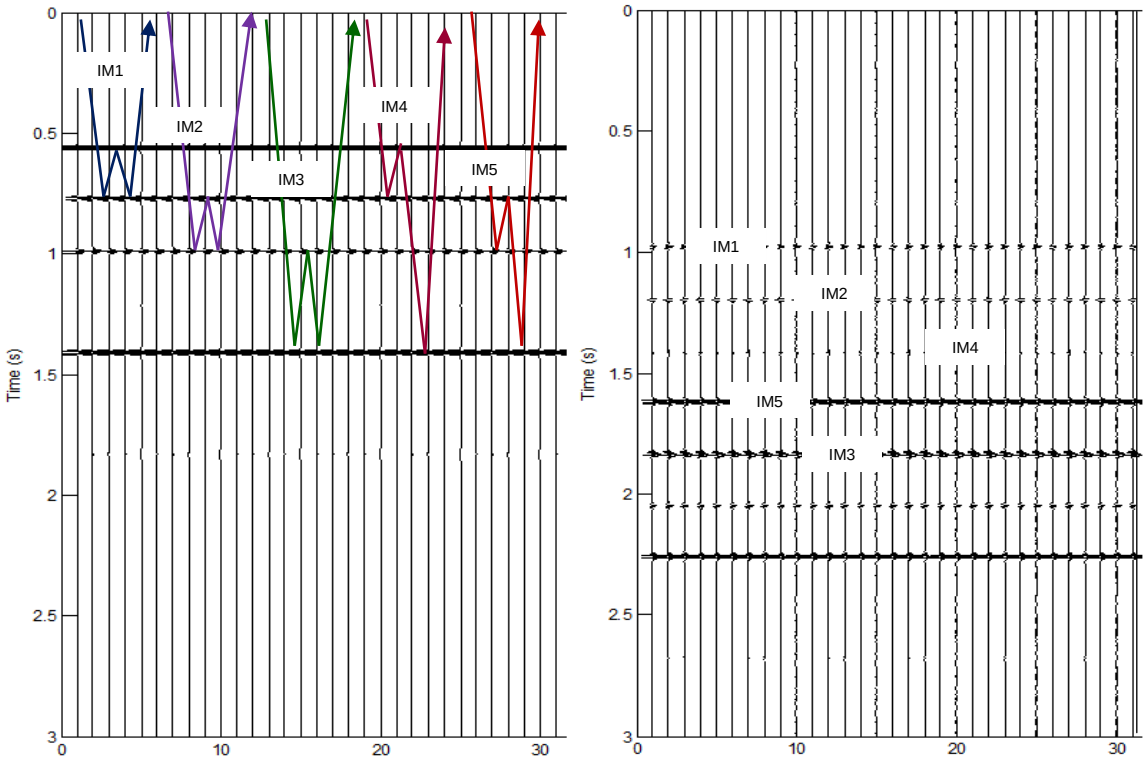

Figure 5.6: Comparison of synthetic model data of the NEBC (left side) and synthetic output prediction (right side).

The first order internal multiple due to the high impedance contrast between Banff and the receiver/source medium arrives at 1.0s, coinciding with the Jean Marie reflector. The strongest internal multiples arrives at 1.6s, is a short-path multiple its amplitude is large due to high contrast of impedance between Jean Marie and Otter Park. This high contrast of impedance between those interfaces is also generating a strong long-path multiple that arrives at 1.83s.

In the Figure 5.7 a comparison between the input synthetic section and input field data is shown. The models are very similar which later allow us to compare the outputs prediction and the arrival times of the internal multiples, Figure 5.9.

5.3 Field data test

The 2D multicomponent land seismic field data set used was provided by Nexen Inc., in this work we only used the P wave. The data itself is high quality (high S/N ratio), and conveniently present internal multiples that are interfering and masking the primary reflections. The source used to acquire this data set was vibroseis, interval sample time of 2ms, receiver interval of 10m, and sources were found every 60m. Sensor Geophysical processed the data, and the processing sequence is presented in the following table. In addition, the first 250ms of this data set was muted because contained noise. Figure 5.10 shows the field data after processing and muting; this data was used as input data.

Conventionally, seismic multiples are removed prior to stacking, in this work we applied the 1D internal multiple attenuation algorithm after the data was stacked for two reasons: 1) since the algorithm works in a 1D medium the input data must be as close as possible to a normal incidence trace, in a flat area an stacked trace is taken to be the response of a normal-incidence reflection at the common midpoint (CMP), besides the stacking process remove the effect of the geometry, and 2) the algorithm is very sensitive to noise or other artefacts that are attenuate with the stacking process.

Table 5.2: Processing sequence applied for Sensor Geophysical

PROCESSING SEQUENCE
Geometry assignment, trace edits and kills
Amplitude recovery: Spherical divergence correction
Singular Value decomposition (SVD) filter to remove ground roll
FK filter to remove surface generated noise
Surface-consistent deconvolution (Spiking)
Prewhitening
Vibroseis Decon compensation
Refraction static corrections, Datum 600 m, Vremp =2200 m/s
Surface-consistent Statics
Surface-consistent Amplitude scaling
T – F Adaptive Noise Suppression, Offset consistent Gain Control
TV Spectral whitening
Normal moveout correction. Front end mute. Automatic gain control
CDP stack
TV Spectral whitening
FK filter to remove surface generated noise
Trace equalization. F-X Filtering. Diffusion filter
FD Time migration. Band pass filter
Trace equalization
Time variant scaling: mean, centre-to-centre, multiple gates

As it was mentioned in previous chapters one of the most important parameters in this technique is the parameter epsilon (ϵ). In order to estimate the value of it an autocorrelation of one trace was performed, see Figure 5.8. Besides, the results of the synthetic model of NEBC also provided a sense of the range that epsilon could be.

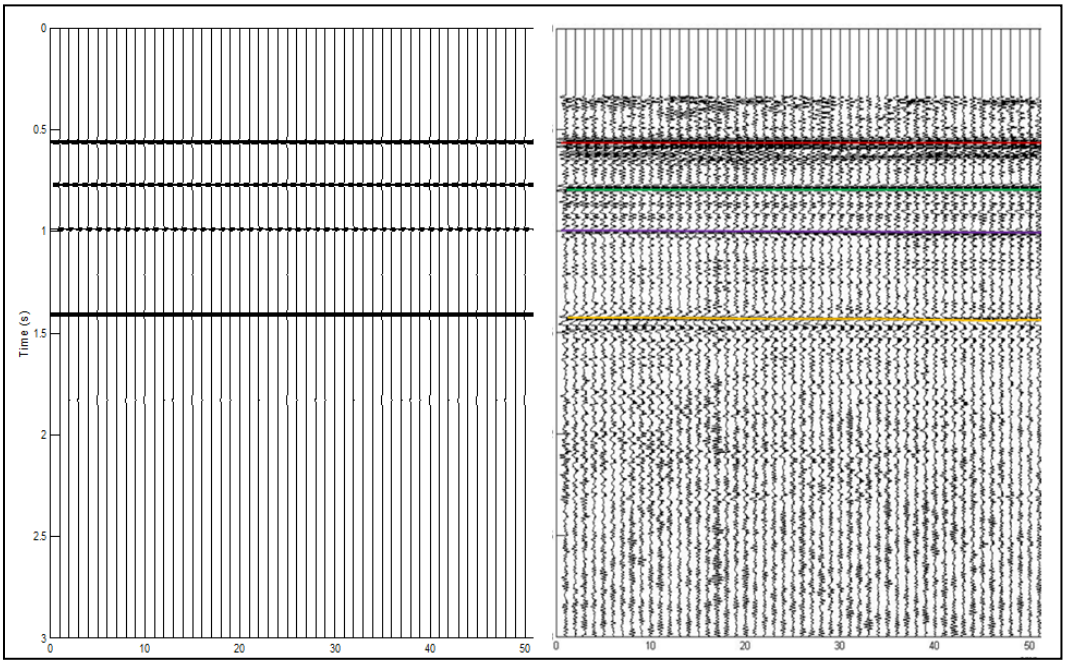

Figure 5.7: Comparison of synthetic model data (left side) and input field data (right side) of the NEBC.

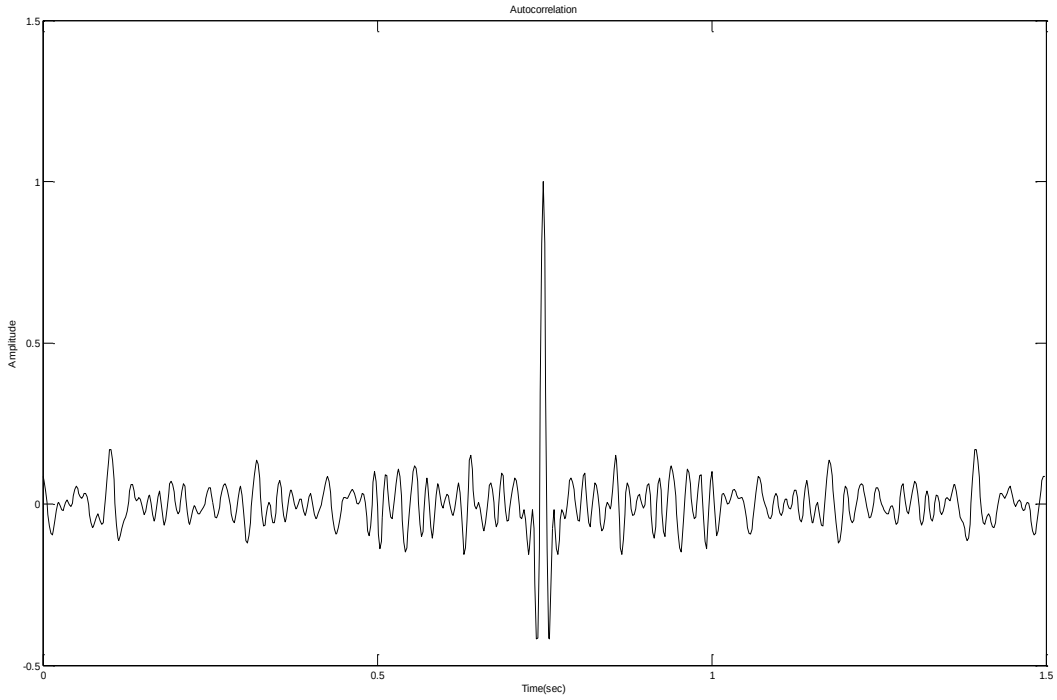

Figure 5.8: Autocorrelation of the input data to estimate epsilon.

Figure 5.9 shows a comparison of the output prediction of the synthetic model and the output prediction of the field data. These two sections point out where the internal multiples could be found. The output prediction present certain amount of noise, however the internal multiples are identified clearly. In Figure 5.11 a prediction output stacked section is shown. Notice this section only contain multiples and noise, but no reflections. The stronger internal multiples arrive around: 1.0s, 1.25s, 1.6s, 1.8s, 1.9s, and 2.1s. The value of epsilon that achieved this prediction was 20 sample points.

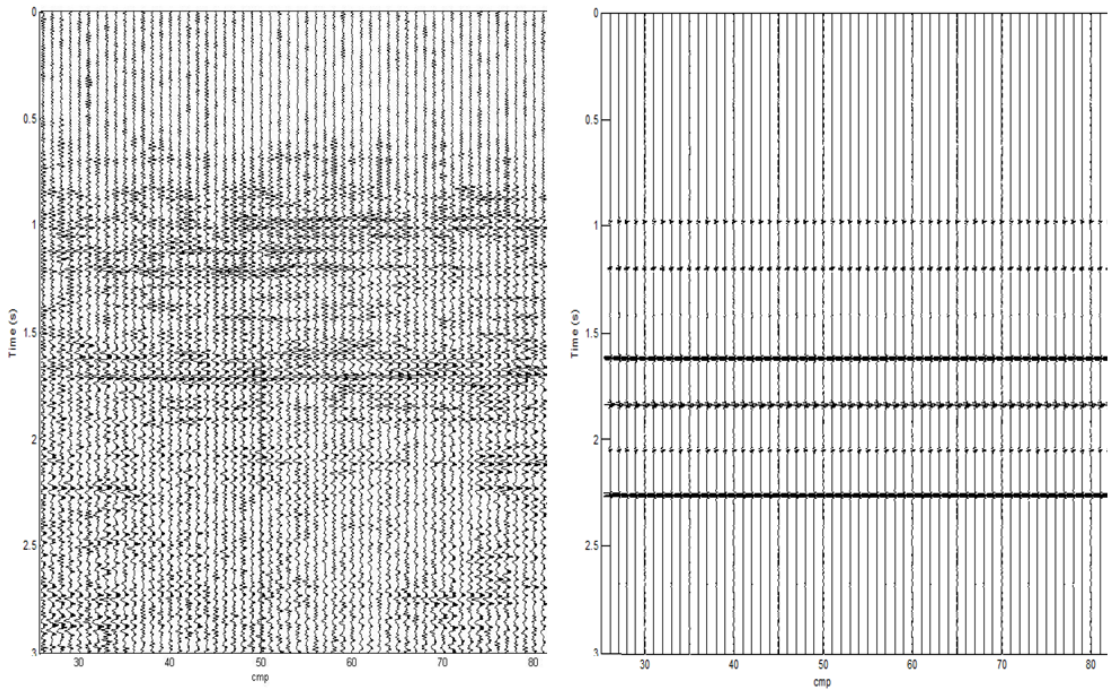

Figure 5.9: Comparison of output prediction of the field data (left side) and output prediction of the synthetic data (right side) of the NEBC.

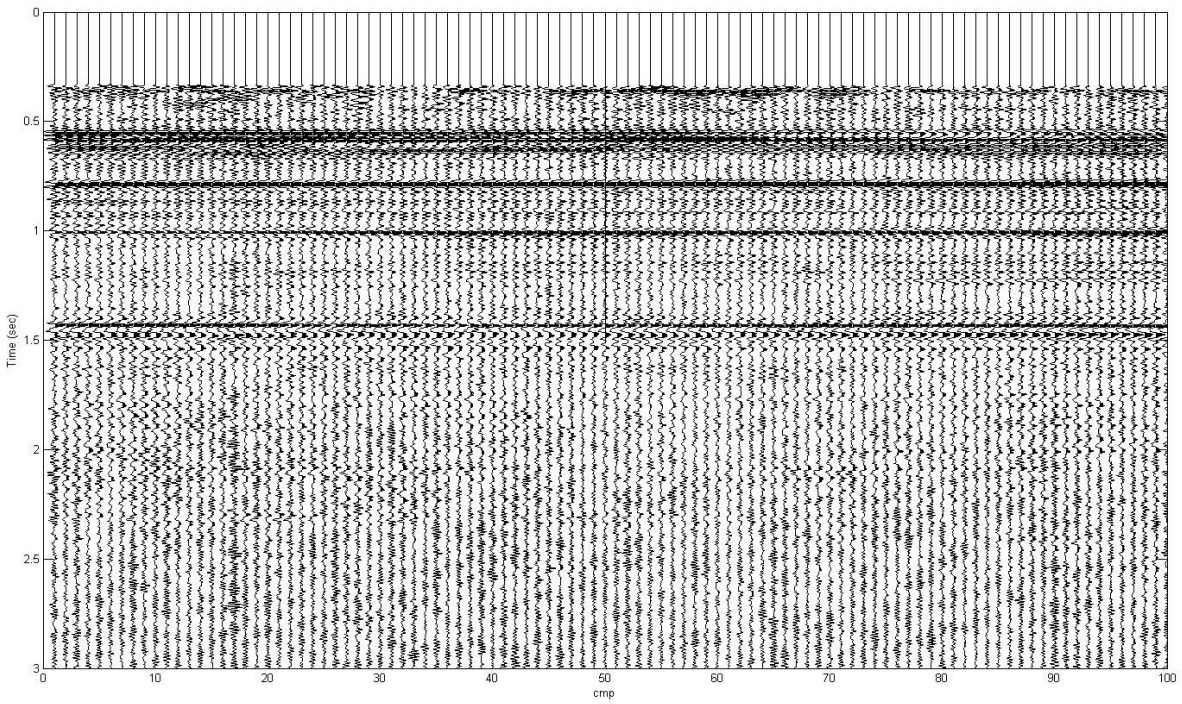

Figure 5.10: Stack section with multiples, after processing, input data.

Figure 5.12 shows a comparison between the input field data and the prediction output, is a zoom of the central part of both sections. Notice that between 0.9s and 1.4s the algorithm predicted the internal multiples that are present in the input data, the times are the same but the amplitude are slightly different. This output prediction section can be considered a map of the places where the internal multiples can be found. Besides, using this technique the analyst can verify if an interbed multiple is interfering with a primary and affecting the amplitude of it, like we show in this chapter. This is very important result because an erroneous value of the amplitude can be very harmful mistake in the application of specialized characterization techniques such as AVO.

As we expected according to the synthetic model of the area, in the output field data prediction there is a first order internal multiple due to the high impedance contrast between Banff and the receiver/source medium that arrives around 1.0s, coinciding with the Jean Marie reflector. Moreover, we identified a strong internal multiples arriving around 1.6s, this is a short-path multiple, its amplitude is large due to high contrast of impedance between Jean Marie and Otter Park. This high contrast of impedance between those interfaces is also generating a strong long-path multiple arriving at 1.83s.

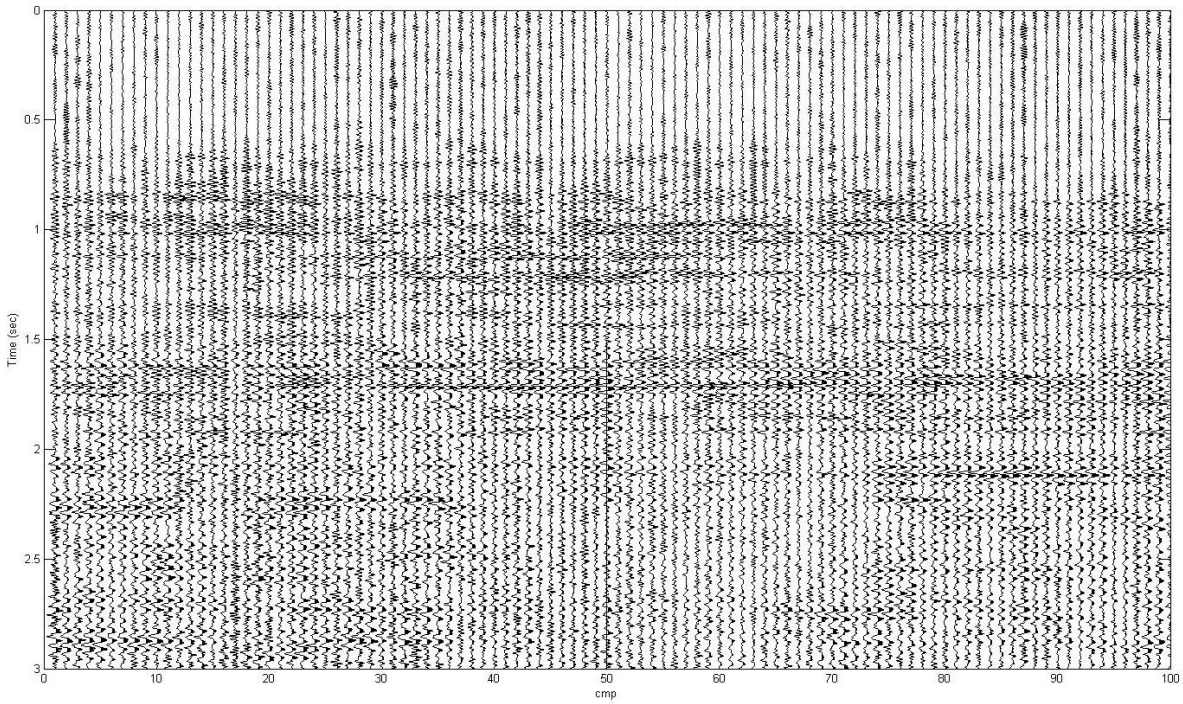

Figure 5.11: Output Prediction full of multiples, stack section

5.4 Summary

In this chapter we presented the results of the application of the internal multiple prediction algorithm on field data. The data is from NEBC. Nexen donated the well log and seismic data information. The well log information allowed us to generate a synthetic seismogram to pre-evaluate around what times the internal multiples can be found based on the combination of the major regional markers or interfaces. Also, we used this synthetic model to pre-estimate the value of the parameter epsilon. The well is 5km away from the 2D seismic line; therefore we adjusted the model for a better match of the marker with principal seismic reflections. The input section contains primary reflections at 0.6s, 0.8s, 1.0s, and 1.43s. The output prediction in shown in Figure 5.10, the output presents noise which makes more difficult to identify the internal multiples, but still there are clear events that arrives at 1.0s, 1.25s, 1.6s, 1.8s, 1.9s, and 2.1s.

The results found are satisfactory; the algorithm predicts internal multiples at the correct times and with approximate amplitudes. The first order internal multiple due to the high impedance contrast between Banff and the receiver/source medium that arrives around 1.0s, coinciding with the Jean Marie reflector. Using this technique the analyst can verify if an interbed multiple is interfering with a primary and affecting the amplitude of it, like we show in this chapter. This output prediction section can be considered a map of the places where the internal multiples can be found.

We identified a strong internal multiples arriving around 1.6s. This is a short-path multiple, its amplitude is large due to high contrast of impedance between Jean Marie and

Otter Park. This high contrast of impedance between those interfaces is also generating a strong long-path multiple arriving at 1.83s. The noise presents in the output section can be removed later in the subtraction process. Using this technique the analyst can verify if an interbed multiple is interfering with a primary and affecting the amplitude of it.

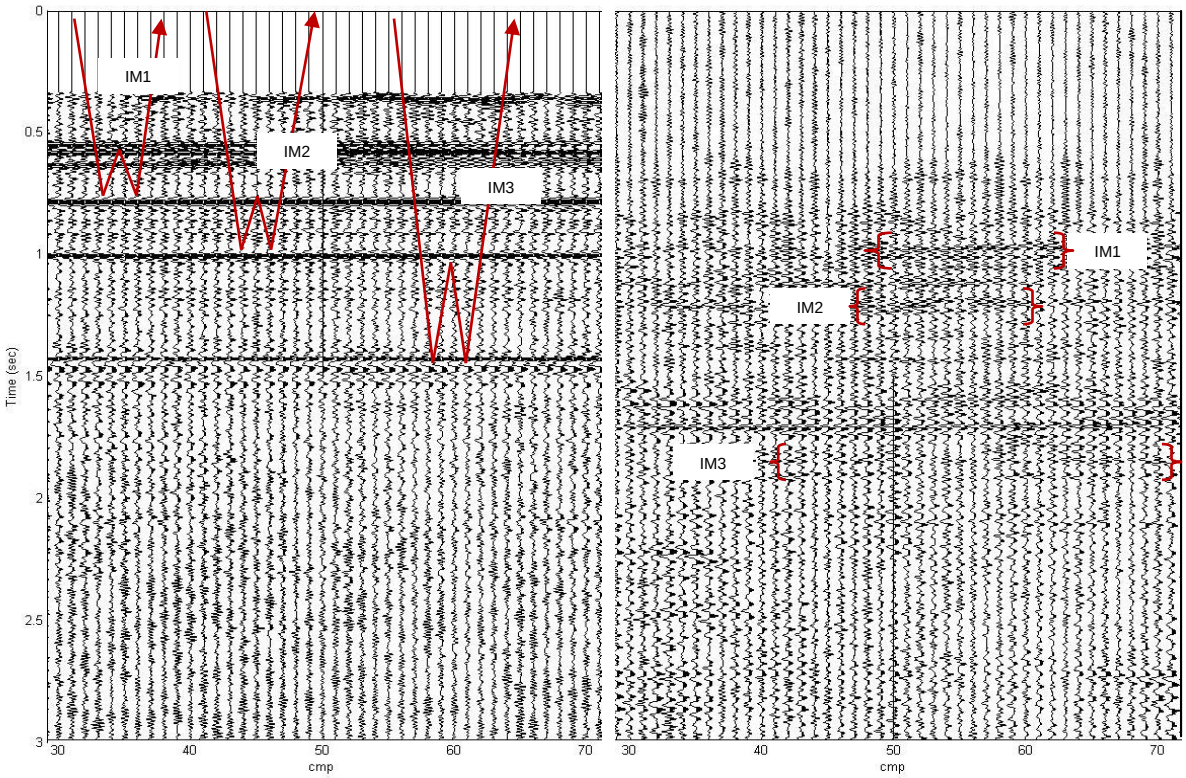

Figure 5.12: This represents a zoom of a time section from NEBC. Left side: Input field data. Right side: Output prediction.

Chapter Six: Conclusions and future work

In the first part of this work we used synthetic data to study the relationship the parameter epsilon in the algorithm and aspects of the data, such as wavelet, central frequency, combination of depths and velocities, and noise. Based on the synthetics experiments performed several conclusions can be drawn:

- For different synthetic models the algorithm works satisfactory, predict multiples in the correct time and the amplitude is similar in synthetic data free of noise.
- The output prediction depends strongly on the parameter epsilon (ϵ). The importance of the parameter epsilon lies in the fact that events are not delta functions, they have an intrinsic form, the width of the wavelet.
- For smaller epsilon values, the algorithm affects the primaries. Therefore, an underestimation of epsilon could damage significantly important information present in the data. An overestimation of the value of epsilon would not damage the data, but the output will not show any internal multiples or other seismic events.
- The components of the wavelet do not affect the prediction of internal multiples using this technique as long as the parameter epsilon is well estimated.
- The algorithm works satisfactory in noisy synthetic data if there is a high contrast of impedance at the bottom reflectors that generate the internal multiple. The algorithm does not show accurate results in noisy data if the internal multiple has small amplitude.

Then, we conducted 2D marine common offset seismic survey in the physical model lab of the University of Calgary. We used the physical model data acquired in a controlled environment with certain quantity of noise to test the algorithm. There is also a high contrast of impedance between materials. The results found indicate that the algorithm predicted multiples at the correct time and similar amplitudes in a high quality data, without any a priori information about the subsurface. Autocorrelation of the input data is recommended to estimate the value of epsilon. Pre-processing of the data is required. The output prediction depends strongly on the parameter epsilon. The value of epsilon (ϵ) that performed the best prediction was 50 (sample points). The output prediction does not affect the primaries. Moreover, the input data and output prediction presents reverberations or ringing effect. A certain amount of seismic energy is not been transmitted from one layer to the next through the water and aluminium layers. It remains trapped within of these layers producing additional arrivals on the section at each rebound. The algorithm is capable of predicts these reverberations.

The experience and knowledge acquired with the application of the algorithm on synthetic data and then physical modeling data allowed us to finally apply the internal multiple attenuation algorithm on field data. The 2D seismic data is high quality, presents strong reflections, low noise, and some internal multiples. Since we are running a 1D version of the algorithm, the input data has been stacked, and muted in order to be as free as possible of noise, because the algorithm is very sensitive to noise. The input section contains primary reflections at 0.6s, 0.8s, 1.0s, and 1.43s. The output prediction presents noise,

however, the internal multiples are identified clearly around 1.0s, 1.25s, 1.6s, 1.8s, 1.9s, and 2.1s. The value of epsilon (ϵ) used was 20 sample points.

Using this technique the analyst can verify if an interbed multiple is interfering with a primary and affecting the amplitude of it. This is very important result because an erroneous value of the amplitude can be very harmful mistake in the application of specialized characterization techniques such as AVO. This output prediction section can be considered a map of the places where the internal multiples can be found.

For future work we recommend the application of adaptive subtraction method to remove the predicted internal multiples from the input data by estimating shaping filters, minimizing the difference or misfit between the input data and the output prediction using least-squares. Moreover, we recommend the application of the algorithm on geological complex seismic data, and developing of a 2D version of the algorithm.

REFERENCES

Aki, K., and Richards, P. G., 1980, Quantitative seismology: Theory and methods. Freeman and Co., New York.

Alvarez, G., and Larner, K., 1996, Implications of multiple suppression for AVO analysis and CMP –stack data. 66th Annual Meeting of the Society of Exploration Geophysicist, Expanded abstracts, p: 1518-1521.

Araujo, F. V., Weglein, A. B., Calvalho, P., and Stolt, R., 1994, Inverse scattering series for multiple attenuation: an example with surface and internal multiple: 64th Annual meeting of the Society of Exploration Geophysics, Expanded Abstracts, 1039–1041.

Backus, M., 1959, Water reverberations, their nature and elimination: Geophysics, **24**, p:233-261.

Cao, Z., 2006, Analysis and application of the randon transform: M.Sc. Thesis, Univ. of Calgary.

Clayton, R., and Stolt, R., 1980, A Born-WKBJ inversion method for acoustic reflection data, Geophysics, Vol. 46, No. 11, p. 1559-1567.

Carvalho, P.M., Weglein, A. B., and Stolt, R. H.,1991, Examples of a nonlinear inversion method based on the T matrix of scattering theory: Application on multiple suppression: 61st Ann. Internat. Mtg., Soc. Expl. Geophys., Expanded Abstracts, 1319-1322.

Coates, R. T., and Weglein, A. B., 1996, Internal multiple attenuation using inverse scattering: Results from prestack 1 & 2D acoustic and elastic synthetics. 66th Ann. Internat. Mtg., Soc. Expl. Geophys., Expanded Abstracts, 1522–1525.

De Hoop, M. V. 1996. Generalization of the Bremmer coupling series. J. Math. Phys., 37, 3246-3282.

Diebold, J., and Stoffa, P., 1981, The traveltime equation, tau-p mapping , and inversion of common midpoint data: Geophysics, 46, 238-254.

Ebrom, D. A., and McDonald, J. A., 1994, Seismic physical modelling: Geophysics reprint series No .15: Society of Exploration Geophysicists, 1–3.

Edwards, D. J., 1992, 3D Modelling of a reef-fault block structure: CREWES Research Report, No. 4.

Fokkema, J. T., and Van den Berg, P. M., 1993, Seismic applications of acoustic reciprocity: Elsevier Science Publ. Co., Inc

Foster, D. J., and Mosher, C., C., 1992, Suppression of multiple reflections using the Radon transform, Geophysics, 57, p: 386-395.

Glass, D.J. 1997. Lexicon of Canadian stratigraphy volume 4 Western Canada, including Eastern British Columbia, Alberta, Saskatchewan and southern Manitoba; Canadian Society of Petroleum Geology, Calgary, p. 1423

Hrabi, K. D., 1994, 3-d physical seismic modelling study of a lower cretaceous channel in southern alberta: M.Sc. Thesis , Univ. of Calgary.

Ikelle, L. T., Amundsen, L., and Eiken, O., 1997, Multiple attenuation at primary/multiple interferences: The trol example: The Leading Edge, , No. 12, 1751–1753.

Jakubowicz, H. 1998. Wave equation prediction and removal of interbed multiples. Expanded Abstracts. Soc. Explor. Geophys, p:1527-1530

Jones, I.F., and Levy, S. 1987, Signal-to-noise ratio enhancement in multichannel seismic data via the Karhunen-Loève transform: Geophysical Prospecting, **35**, 12-32.

Kennett, B. L.N., 1979, The suppression of surface multiples on seismic records: Geophys. Prosp., **27**, 484–600.

Lawton, D. C., Margrave, G. F., and Gallant, E. V., 1998, Physical modelling of anisotropic thrust: CREWES Research Report.

Lippmann, B. A., & Schwinger, J. 1950. Variational principles for scattering processes I. Phys. Rev., 79(3), 469-480.

Lippmann, B. A. 1956. Rearrangement Collisions. Phys. Rev., 102(1), 264-268.

Mahmoundian, F., Margrave, G., Daley, P. F., Wong, J., and Gallant, E., 2011, Determinig elastic constants of an orthorhombic material by physical seismic modeling: CREWES Research Report.

Matson, K., 1996, The relationship between scattering theory and the primaries and multiples of reflection seismic data, Journal of Seismic Exploration, Vol. 5, p. 63-78.

Matson, K., 1997, An inverse scattering series method for attenuating elastic multiples from multicomponent land and ocean bottom seismic data. PhD Thesis, University of British Columbia.

Matson, K. H., Pascal, D., and Weglein, A. B., 1999, A comparison of three multiple attenuation methods applied to a hard water-bottom data set: The Leading Egde, , No. 18, 120–126.

Malcom, A., 2005, Data continuation for data regularization and internal multiples. PhD Thesis. Colorado School of Mines.

Margrave, G. F., 1999, The methods of seismic data processing: Department of Geology and Geophysics, University of Calgary.

Moses, H. E. 1956, Calculation of scattering potential from reflection coefficients. Phys.Rev., p:102, 559-567.

Nita, B. G., and Weglein, A. B., 2007, Inverse scattering internal multiple attenuation algorithm: an analysis of the pseudo-depth and time monotonicity requirements. SEG Annual Meeting. P:2461-2465.

Nita, B. G., and Weglein, A. B.,2009, Pseudo-Depth/Intercept Time Monotonicity Requirements in the Inverse Scattering Algorithm for Predicting Internal Multiple Reflections. Communications in Computational Physics. Vol. **5**, No. 1, p: 163-182.

Prosser, R. T., 1969, Formal solutions of inverse scattering problems. Journal of Math. Phys., 10, 1819-1822.

Razavy, M. 1975. Determination of the wave velocity in an inhomogeneous medium from the reflection coefficient. Journal Acoustic Society of America, 58, 956-963.

Sloat, John. 1948. Identification of echo reflections. Geophysics, 13(1), 27-35.

Stolt, R. H., and Jacobs, A., 1980, An approach to the inverse seismic problem: Submitted to Geophysics.

Taylor, J. R., 1972, Scattering Theory: New York, Jonh Wiley & Sons, Inc.

Telford, W.M., Geldart, L.P., and Sheriff, R.E., 1990, Applied Geophysics. Second Edition. Cambridge University Press. p: 136-206.

Treitel, S., Gutowski, P. R., and Wagner, D. E., 1982, Plane-wave decomposition of seismograms: Geophysics, **47**, no. 10, 1375-1401.

Trinks, I., 2000, removing multiples from the wide-angle wavefield. Lithos Science report, p: 113-116.

Verschuur, D. J., Herrman, P., Kinneging, N.A., Wapenaar, C. P. A., and Berkhout, A. J., 1988, Elimination of surface-related multiple reflected and converted waves: 58th Annual meeting of the Society of Exploration Geophysicist, Expanded abstracts, 1017-1020.

Verschuur, D. J., Berkhout, A. J. and Wapenaar, C. P. A., Adaptive surface-related multiple elimination, *Geophysics*, 57, 1166-1177, 1992

Verschuur, D.J., 1992, Surface-related multiple elimination in terms of Huygens' sources, Journal of seismic exploration, **1**, 49-59.

Verschuur, D. J., 1991, Surface-related multiple elimination: and inverse approach: PhD. Thesis, Delft University of Technology.

Weglein, A.B., Boyse, W.E., and Anderson, J. E., 1981, Obtaining 3D velocity information directly from reflection seismic data: An inverse scattering formalism: Geophysics, 46, 1116-1120.

Weglein, A. B., 1985, The inverse scattering concept and its seismic application, *in* Fitch, A. A., Ed., Developments in geophysical exploration methods: Elsevier Science Publ. Co., Inc., **6**, 111–138.

Weglein, A. B., F. A. Gasparotto, P. M. Carvalho, and R. H. Stolt, 1992, Nonlinear Inverse Scattering for Multiple Suppression: Application to Real Data. Part I. (*1992*). SEC Expanded Abstracts. pp 1093-1095.

Weglein, A. B., F. A. Gasparotto, P. M. Carvalho, and R. H. Stolt, 1997, An inverse scattering series method for attenuating multiples in seismic reflection data: Geophysics, 62, 1975–1989

Weglein, A. B., and Matson, K. H., 1998, Inverse scattering internal multiple attenuation: analytic example and subevent interpretation: Part of SPIE Conference on Mathematical Methods in Geophysical Imaging V, 3453.

Weglein, A., Araujo, F. B., Carvalho, P. M., Stolt, R. H., Matson, K. H., Coates, R. T., Corrigan, D., Foster, D. J., Shaw, S. A., & Zhang, H., 2003. Inverse scattering series and seismic exploration. Inverse Problems, 19, R27-R83.

Weglein, A. B., Araujo, F. V., Carvalho, P., Stolt, R., Matson, K., Croates, R., Dennis, C., Foster, D., Shaw, S.,and Zang, H., 2001, Inverse scattering series and seismic exploration: Inverse Problems, 19, 1217–1225.

Weglein, A. and W. Dragoset, eds., 2005, Multiple attenuation: SEG Geophysics Reprint Series.

Wong, J., Hall, K. W., Gallant, E. V., Maier, R., Bertram, M. B., and Lawton, D. C., 2009, Seismic physical modelling at the University of Calgary: CSEG RECORDER, No. 3, 36–43.

Yan, Y., 2002, Supression of water-column multiples by combining components of ocean-bottom seismic surveys. MSc Thesis. University of Calgary.

Yilmaz, O. 1987. Seismic data processing. Investigations in Geophysics, vol. 2. Tulsa: Society of Exploration Geophysicists.

Xiao, C., Bancroft, J., Brown, J., and Cao, Z., 2003, Multiple suppression: A literature review: Crewes Report, 15.

Zuleta, L., 2012, Near-surface characterization and Vp/Vs analysis of a shale gas basin. MSc. Thesis. University of Calgary.